B.O.N.G.I.

Biological Observation and Navigation for Guano Investigation

A remotely operated robotic system for non-invasive monitoring of African penguins during moult

Prepared by:
Rachael Guise-Brown (GSBRAC001),
Kavya Kaushik (KSHKAV001),
Heinrich Crous (CRSHEI004)

Prepared for:
EEE4113F
Department of Electrical Engineering
University of Cape Town

May 25, 2025

Declaration

1. I know that plagiarism is wrong. Plagiarism is to use another's work and pretend that it is one's own.
2. I have used the IEEE convention for citation and referencing. Each contribution to, and quotation in, this report from the work(s) of other people has been attributed, and has been cited and referenced.
3. This report is my own work.
4. I have not allowed, and will not allow, anyone to copy my work with the intention of passing it off as their own work or part thereof.

Rachael Guise-Brown,

Kavya Kaushik,

Heinrich Crous,

May 25, 2025

Name Surname

Date

Abstract

Nam dui ligula, fringilla a, euismod sodales, sollicitudin vel, wisi. Morbi auctor lorem non justo. Nam lacus libero, pretium at, lobortis vitae, ultricies et, tellus. Donec aliquet, tortor sed accumsan bibendum, erat ligula aliquet magna, vitae ornare odio metus a mi. Morbi ac orci et nisl hendrerit mollis. Suspendisse ut massa. Cras nec ante. Pellentesque a nulla. Cum sociis natoque penatibus et magnis dis parturient montes, nascetur ridiculus mus. Aliquam tincidunt urna. Nulla ullamcorper vestibulum turpis. Pellentesque cursus luctus mauris.

Nulla malesuada porttitor diam. Donec felis erat, congue non, volutpat at, tincidunt tristique, libero. Vivamus viverra fermentum felis. Donec nonummy pellentesque ante. Phasellus adipiscing semper elit. Proin fermentum massa ac quam. Sed diam turpis, molestie vitae, placerat a, molestie nec, leo. Maecenas lacinia. Nam ipsum ligula, eleifend at, accumsan nec, suscipit a, ipsum. Morbi blandit ligula feugiat magna. Nunc eleifend consequat lorem. Sed lacinia nulla vitae enim. Pellentesque tincidunt purus vel magna. Integer non enim. Praesent euismod nunc eu purus. Donec bibendum quam in tellus. Nullam cursus pulvinar lectus. Donec et mi. Nam vulputate metus eu enim. Vestibulum pellentesque felis eu massa.

Quisque ullamcorper placerat ipsum. Cras nibh. Morbi vel justo vitae lacus tincidunt ultrices. Lorem ipsum dolor sit amet, consectetuer adipiscing elit. In hac habitasse platea dictumst. Integer tempus convallis augue. Etiam facilisis. Nunc elementum fermentum wisi. Aenean placerat. Ut imperdiet, enim sed gravida sollicitudin, felis odio placerat quam, ac pulvinar elit purus eget enim. Nunc vitae tortor. Proin tempus nibh sit amet nisl. Vivamus quis tortor vitae risus porta vehicula.

Contents

List of Figures

Chapter 1

Introduction

African Penguins (Spheniscus demersus), once widespread along the southern African coastline, have been officially classified as critically endangered as of 2024. The sharp decline in their population is primarily due to diminishing fish stocks, habitat degradation, and increased predation. Recognising the urgent need for conservation innovation, the 2025 EEE4113F Design Class was tasked with developing technological solutions to support the protection and recovery of this iconic species.

1.1 Background

This design project was informed by collaboration with two leading ornithologists—Dr. Alistair McInnes and Christina Hagen—each of whom presented a unique challenge faced in the ongoing effort to conserve African Penguins. Dr. McInnes focuses on the moulting period—a critical 21-day phase during which penguins are land-bound and unable to feed, making them vulnerable to starvation and stress. Since the birds cannot be handled during this phase, non-invasive monitoring technologies are essential to assess their health and behaviour. Christina Hagen is establishing a new penguin colony at De Hoop Nature Reserve, chosen for its food availability. However, predators—including caracal, leopard and especially honey badgers—pose a major threat. Her challenge is to deter predators without harming either the penguins or the wildlife.

1.2 Problem Analysis

This project began with a human-centred design process led by the Design School (D-School), where we explored the problem space through a client-focused lens. This approach encouraged us to understand the broader context of the problem spaces, enabling the development of functional solutions that are also considerate of real-world environments.

After considering both conservation challenges, our team focused on Dr. McInnes's problem of non-invasively monitoring moulting penguins. Several potential approaches were explored during the problem definition and ideation phases including: automated scales to track body mass changes as a health indicator, remote-controlled cameras to visually assess moult stages and physiological monitoring tools, such as temperature sensors. Further research (see Section 2) revealed that penguin faecal matter provides reliable insights into stress and physiological health. Since direct collection by researchers is not allowed, we proposed a remotely operated robot to gather faecal samples non-invasively—enabling effective monitoring without disturbing the penguins.

1.3 System Requirements

The user requirments for this system are detailed in Table 1.1

Table 1.1: Overall User Requirements

UR01	**Remote Operation for Sample Collection:** The system must allow the ornithology department to remotely control the device to locate and collect penguin fecal samples without direct human interaction.
UR02	**Visual Monitoring Capability:** The system must provide the ornithology department with a live video feed of the environment to aid in navigation and sample identification.
UR03	**Cordless Operation for Mobility:** The system must operate wirelessly for a sufficient duration to allow for sample collection within the penguin enclosure.
UR04	**Sample Collection Mechanism:** The system must incorporate a mechanism capable of collecting fecal samples without contaminating them.
UR05	**Sample Storage:** The system must be able to hold the collected sample to carry back to be tested.
UR06	**Robustness for the Environment:** The system must be robust enough to operate reliably within the penguin environment.
UR07	**Ease of Use for Ornithologists:** The control interface and sample retrieval process should be intuitive and easy for the ornithology department to use.
UR08	**Budgetary Constraints:** The system must be developed and operated within the allocated project budget of R1500 for the whole system.

1.4 Scope & Limitations

The system is intended for use at the Betty's Bay colony, where moulting penguins typically remain on a concrete slipway. It is designed to operate on the slipway's uneven but firm surface and is not required to navigate sand, rocks, or rugged terrain. Its use is limited to areas where penguins are stationary and can be observed from a distance.

1.5 Subsystem Breakdown

This project consists of the following subsystems.

- **Chassis and Scraper Subsystem:** Provides the structural base of the robot, housing internal components in a sealed, 3D-printed chassis. It includes a front-mounted, servo-driven scraper for non-invasive surface sample collection.
- **Electrical Subsystem:** Built around the ESP32-CAM, it controls all servos and motors, manages power distribution, and facilitates internal communication between components.
- **Software Subsystem:** Enables remote control of movement and scraping via a user interface. It supports live video streaming and is designed for future mobile compatibility.

Chapter 2

Literature Review

The African Penguin (Spheniscus demersus) has recently become critically endangered [1]. Therefore, increased monitoring is required to protect this species. Moulting is a critical phase in their life cycle, during which they are particularly vulnerable. Accurate health monitoring is, therefore, essential for conservation efforts. This literature review explores the complexities of the moulting process, the factors that influence penguin health during this time, and the various techniques used to monitor them. It further highlights the necessity of non-invasive monitoring methods to reduce stress and improve the reliability of data.

2.1 Understanding the Moulting Process in African Penguins

Moulting is a process that is unique among birds. During moult, birds partially or completely replace their feathers. Unlike most avian species, the endangered African Penguin (Spheniscus demersus) experiences a complete, annual feather replacement – shedding their entire plumage at once. This is known as a "catastrophic moult [2]. Penguins' feathers wear from saltwater, UV exposure, and abrasion. Therefore, to maintain insulation and waterproofing, moulting is essential for survival in cold, marine environments [2]. Furthermore, poor feather condition reduces their foraging ability [3]. The moulting process is divided into three main phases: pre-moult, moult, and post-moult [4].

2.1.1 The Pre-moult Phase

Penguins cannot forage or feed during moult; therefore, the pre-moult fattening period is essential [2]. The pre-moult phase typically occurs after breeding and lasts approximately 34 days [4].

During this phase, penguins must gain weight [2]. They exhibit intense foraging behaviour and increased food intake prior to moult, allowing for rapid fat accumulation [5]. To gain sufficient weight, penguins focus on high-energy prey like sardines and anchovies [4]. Furthermore, they must spend increased time at sea and endure longer foraging trips. These trips can vary depending on their individual condition and food availability [3]. There are some key indicators that a penguin is in the pre-moult phase: their plumage is dense and intact, and their body mass is significantly higher than usual [2].

2.1.2 The Moulting Phase

The moulting phase lasts approximately 21 days [4]. Since penguins are unable to feed during the moulting phase, they experience significant weight loss [2][3]. As previously mentioned, penguins fast

during the moulting phase. Fat accumulated during the pre-moult phase becomes their primary energy source [2]. They do, however, also experience some protein and water loss during this phase [5].

During the moulting phase, penguins remain on land and are sedentary. Their feathers shed progressively [2]. The moulting phase varies across regions. For example, African penguins in South Africa start the moulting phase between September and January while African penguins in Namibia start this phase between April and May [4].

2.1.3 The Post-moult Phase

If a penguin survives the moulting-phase, they must regain their condition during the post-moult recovery phase [4]. The post-moult phase lasts approximately 41 days [4]. During this phase, penguins forage intensively to restore their energy reserves [4]. The timing of the moulting phase directly correlates to the next breeding cycle [4].

Disruptions in the Moulting Process: Signs and Symptoms There are various signs of abnormal moulting. Since the moulting process is essential for the survival of penguins, researchers and conservationists are eager to identify these signs [6]. The consequences of abnormal moulting are catastrophic – especially for the endangered African penguin: higher risk of mortality, greater chick loss, poor post-moult recovery, and significantly reduced breeding success [6][3]. These factors will also be discussed in Section 2.2.

Table 2.1: Signs and Symptoms of Abnormal Molting

External/Physical Signs	**Physiological Symptoms**	**Behavioural Indicators**
Delayed moult onset compared to the normal seasonal window [6]	Abnormally low red blood cell count during moult [5]	Sedentary for extended periods beyond the normal moult duration [6]
Moulting outside of the usual location or season [7]	Abnormally high corticosterone during moult [5]	Lethargy or reduced activity [6]
Incomplete moult: patches of old feathers remain [6]	Poor thermoregulation due to insufficient feather coverage [6]	Failure to rejoin the group post-moult (social isolation) [6]
Poor feather regrowth or uneven replacement [1]	Loss of waterproofing, leading to hypothermia if entering water [3]	Refusal or inability to forage post-moult due to their poor physical condition [7]
Moulting for longer than the usual moulting period, i.e., longer than 21 days [1]		
Low pre-moult weight at the start of the moulting phase [6]		

2.1.4 Root Causes of Moulting Irregularities in African Penguins

Understanding the root causes behind moulting irregularities is just as important as identifying the signs and symptoms of an abnormal moult. Researchers and conservationists must consider these factors holistically to effectively address the issue [6][3].

Moulting irregularities can occur due to various reasons: nutritional and energetic stress, hormonal and biological factors, or environmental and climatic stressors.

2.1.5 Nutritional and Energetic Stress

Penguins may experience nutritional and energetic stress mainly due to inadequate pre-moult fattening [6]. This can occur due to poor prey quality (for example, low sardine biomass), competition with fisheries, or climate change leading to low food availability [8][3]. Consequently, penguins might have insufficient energy stores for a complete moult [7].

2.1.6 Hormonal and Biological Factors

Hormonal imbalances (especially thyroid and sex hormones) interfere with moult onset and progression and are more common among older penguins [6]. Therefore, older birds are more prone to moulting abnormalities [6].

2.1.7 Environmental and Climatic Stressors

Climate change, leading to temperature extremes and heat stress, affects penguins' ability to successfully moult [1][3]. Furthermore, it may contribute to habitat degradation which exposes penguins during the vulnerable moulting phase [9]. Finally, rain or flooding can damage nests and interrupt the breeding-to-moult transition [3].

2.2 Important health factors to consider during the moulting process of African Penguins

Various physiological systems of the penguin's body are affected during the moulting process, including weight and body mass changes, hormonal and metabolic changes, and specific biochemical alterations. This section focuses on the key health indicators identified in the review that directly impact the moulting process of the African penguin.

2.2.1 Weight and Body mass

The change in the weight and body mass of moulting penguins is the most significant and consistent factor observed across all studies. The change in the weight and body mass of moulting penguins is the most significant and consistent factor observed across all studies. According to Cooper [2], pre-moult penguins gain up to 31% more than breeding penguins, which can be approximated as their mass gain before they moult. They lose up to 41% of their body mass during the moult with fat loss being the highest at 56%, water loss at 45% and protein loss at 42%.

An important consideration is mentioned by Lewis [10] which indicates that caged birds suffer through higher body weight loss because of their increased stress levels, therefore showing the direct impact of invasive monitoring techniques. Weight monitoring can play a strong and measurable role in monitoring penguin health; however, it is important to factor in the impact of invasive monitoring on weight loss which is the most common method identified across current literature.

2.2.2 Hormonal and stress markers

There are significant hormonal changes that can be observed in the penguins' bodies which are key indicators of psychological strain. Mazzaro et al [5] found lower than baseline corticosterone levels in the captive penguins' bodies before and after the moulting process, which is present to prevent protein degradation and inhibition of feather formation. Driscoll et al. [11] further establish that this decrease is a real psychological occurrence even in wild penguins. They validated the use of Fecal Glucocorticoid Metabolites (FGMs) as bio-markers of stress, dropping from 85 ng/g to 20 ng/g over a three-week moulting period for field penguins. These levels can be a good indicator when monitoring the moulting process by analysing the internal stress patterns that occur because of the fat loss in the penguins' bodies. This monitoring method is further discussed in Section 2.3.3

Besides moulting phases, elements like age, sex and reproductive conditions also influence hormonal levels and should be considered as important factors for when observing hormonal markers [1].

2.2.3 Diseases and Parasites

The penguins are at a higher risk of contracting diseases due to their suppressed immune system during the moulting process. Parsons et al. [12] identified common parasites like Babesia, Mycoplasma and Borrelia, with Babesia-infection noted as the one of the most severe, as it results in abnormalities in erythrocyte size, triggers an active inflammatory response and impairs hepatic function. Birds that undergo incomplete moulting because of inadequate pre-moult weight gain are more susceptible to these pathogens [11].These symptoms are not always visible but significantly affect the birds' metabolic function which is an added stressor given the high-energy demands during moulting [12].

Descriptive statistical analysis conducted by Austin [6] indicates that normally moulted birds had lower incidences of illnesses within six months of moulting compared to birds that experienced abnormal moulting. While most diagnosis of the diseases requires blood sampling, early detection of these symptoms can significantly improve intervention outcomes. Visible outcomes such as sudden behavioural changes, as listed in Table 2.1 can be be used as indicators of underlying diseases in the penguins.

2.2.4 Blood based health indicators (Haematology and Biochemistry)

Blood analysis conducted by various studies across the review indicate significant changes covering hematologic and biochemical markers indicative of the health conditions of moulting penguins.

Mazarro et al [5] observed significant decrease in haematocrit and red blood cell counts during moulting because of the physical strain endured by the penguins during the moulting process. Parson et al. [12] conducted a study that provides baseline hormonal values for wild penguins, which indicate that male penguins have higher haematocrit, and red cell counts while female penguins have higher calcium and phosphate in their bodies.

Biochemical shifts observed during the moulting process include significant declines in protein, glucose, and lipid levels, indicating a depletion of energy reserves. Additionally, the study conducted by Parson et al. [13] highlighted regional variance with Western Cape penguins having higher cholesterol and low albumin to globulin ratios; suggesting higher stress levels.

These indicators, which are obtained through invasive blood sampling techniques, play an important role in understanding the physiological changes that take place in moulting penguins. These indicators can serve as baseline values to interpret weight changes and hormonal fluctuations during moulting.

2.3 Health Monitoring Techniques

While numerous methods exist for measuring body composition in birds, many are not suitable for research on live subjects due to their invasive nature. Traditional techniques often require the bird to be anesthetized or deceased to obtain accurate measurements [14]. For example, various analytical chemistry procedures are considered the 'gold standard' for measuring fat, water, and protein content, but these necessitate destructive sampling [14]. Although such methods can provide precise results, they preclude the possibility of longitudinal studies on individual animals and raise ethical concerns regarding animal welfare.

Recognizing the limitations of fully invasive techniques, researchers have also explored methods that, while requiring capture, offer valuable insights into avian health and condition with less drastic intervention. These methods often involve temporary capture for specific measurements or sample collection, providing a balance between minimizing disturbance and gathering essential data. This section will explore several of these methods, noting that while the measurement itself may not be invasive, the process of obtaining it necessitates some level of interaction with the animal.

2.3.1 Assessment of Body Condition and Composition

In birds, the most common way to measure protein reserves is through breast muscle thickness. Sears developed a method to measure the breast muscle thickness of live birds using ultrasound, as well as a colour-based fat scoring system to estimate subcutaneous fat levels [15]. The method was tested on the Mute Swan and validated against other measures of protein and fat reserves showing that the results were accurate and repeatable. However, this method requires the capture of the bird to place the ultrasound probe on the bird. This was possible because the Mute Swan is described as easy to catch[15].

Recognizing the limitations of methods relying solely on body mass or body mass ratios, Korine et al. explored the use of dual-energy X-ray absorptiometry (DXA) to more accurately measure fat mass in small birds [16]. This technique utilizes X-rays at two energy levels to differentiate between tissue types, providing a quantitative assessment of fat content. The study highlighted that traditional methods can be problematic as they don't truly account for body composition, and visual estimates of fat reserves are subjective, such as Sears who uses subjective visual methods to determine fat reserves [15]. By using DXA on small birds the study demonstrated a precise and accurate method for measuring fat mass [16]. While requiring capture and potentially invasive techniques to keep the subject stationary for the procedure, DXA offers a more objective and quantitative measure compared to visual scoring or body mass indices.

Guglielmo et al. [17] further addressed the need for precise and non-invasive body composition analysis by evaluating quantitative magnetic resonance (QMR). Recognizing that an ideal technology should rapidly measure fat, lean mass, and total water in non-anesthetized subjects, the study utilized QMR

on three small bird species. This method allows for direct measurement of fat, lean mass, and total water in live, conscious birds [17]. Validated against gravimetric chemical analysis, QMR proved to be a precise and accurate tool, offering significant advancement over traditional methods for monitoring avian body composition in various ecological, physiological, and behavioural studies.

2.3.2 Haematological and Biochemical Analysis

Haematological and biochemical analyses provide direct measures of physiological health. Two studies were done by Parsons et al. [13] and Mazzaro et al. [5] focusing on using this analysis in African Penguins to determine their health.

Parsons et al. focused on establishing baseline haematology and biochemistry parameters in wild adult African penguins, which is the first time this has been reported [13]. Such studies are essential for understanding the normal physiological ranges and for detecting deviations due to disease or environmental factors.

Similarly, Mazzaro et al. examined moult-associated changes in haematologic and plasma biochemical values in African penguins. This study was done on captive penguins and showed the physiological condition, and stress changes that penguins undergo during moult; however, this did not show that blood samples can be used to determine an individual's condition during moult [5]. These studies require the capture of penguins and the collection of blood samples, which, while show the stress African penguins undergo during moult, are invasive and have not been proven to show an individual's condition.

2.3.3 Hormone Monitoring using Faecal Matter

Endocrine monitoring provides insight into the physiological responses of animals to stressors. Driscoll et al. (2023) [11] explored faecal glucocorticoid analysis as a health monitoring tool for endangered African penguins. Faecal samples were collected from penguins throughout their natural lifecycle, including moult, where measurable changes in FGM levels occurred [11]. Driscoll et al. also showed that FGM levels varied between the moult weeks showing that the different stages of moult can also be monitored through changes in FGM [11].

One very interesting case the study highlighted was a penguin, who had no history of abnormal moulting, but abnormally moulted during the study. This showed that deviations from the expected FGM patterns during moult, such as persistently high or erratic levels, could indicate abnormal moult conditions or underlying health issues affecting the penguin's stress response [11]. These results indicate that FGM analysis can detect physiologically meaningful changes in endocrine activity in African penguins [11] and although tested in aquaria can be used to monitor health for penguins in the wild. FGM is a less invasive way of assessing stress responses compared to blood sampling, but it still often requires the capture of penguins to ensure sample collection or relies on collecting samples from known individuals in a controlled setting.

2.4 Non-Invasive Weight Monitoring Techniques for African Penguins.

Using non-invasive methods is important when monitoring the moult of African penguins to reduce the risk of increasing stress levels during this period as discussed in Section 2.1.4. Several technologies and methods have been explored for this purpose.

2.4.1 Perch Scales

For smaller birds, perch scales have been developed to monitor weight changes. Claffy [18] described a small bird perch scale designed to record weight values without the need for handling. A device was developed at the North Carolina Zoologcial Park to monitor the weights of the North American Wood Warblers. Their device was very simply designed with three components: a perch with a scale, a beam sensor and a display, which came to a total cost of $600. Their device has been successfully used to monitor the weights of various birds in captivity for three years without handling [18]. One of the challenges of weighing birds in the wild is getting the bird onto the scale. They were able to overcome this by using food as an incentive [18]. Although this study focuses on smaller birds that fly and use perches, the design concept could possibly be applied to penguins with adjustments.

2.4.2 Automated Weighing Systems

Automated weighing systems offer a promising option for non-invasive weight monitoring in the wild and address the limitations of the perch scale, which was designed for captive birds. Larios et al. [19] detailed the development of an automatic weighting system for wild animals using artificial neural networks. A smart nest box was developed with RFID identification, weight sensors and a camera, allowing for non-intrusive, continuous data collection [19].

Larios et al. addressed two important challenges which are faced by the autonomous weighing of birds in the wild. The first is that animals produce unstable measurement due to movement on the scale, the solution is further discussed in Section 2.6.2. The second challenge is to be able to calibrate the scale while in the wild. The accuracy of measurements was increased by calibrating the scale by taking weight measurements when there is nothing on the scale and so it is continuously calibrated throughout the monitoring process [19]. Additionally, the system was designed for a low-resource environment with low power and low bandwidth, which is important for continuous real-time monitoring in the wild. Their system was tested on the Lesser Kestrel and showed that it is possible to non-invasively monitor their weight changes [19]. While their study focused on different species, the underlying technology could potentially be adapted for penguins, particularly in controlled environments or at specific locations where penguins frequently pass, such as at colony entrances.

An automated weighing system was developed to study the Adélie Penguins by Kerry et al. [20] Their system addressed the limitations of the system developed by Larios et al. [19] and accommodated for the aspects required for penguins. The system developed by Kerry at al. automatically weighs, identifies and determines the direction of penguins moving between their colony and the sea. The colonies were “semi-isolated” with a fence placed around them and a singular gateway to the ocean with the weighbridge system [20]. Figure 2.1 shows how the system was implemented in the colony.

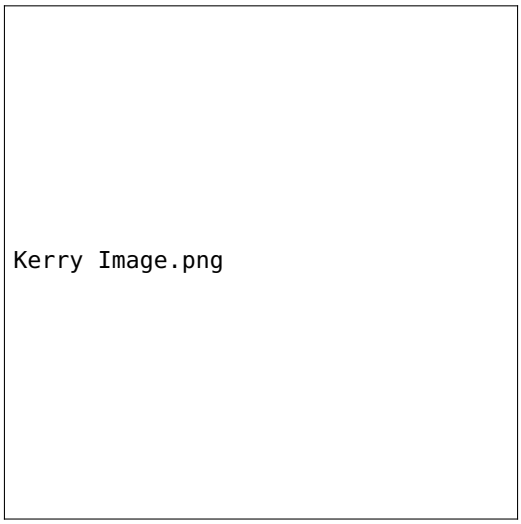

Figure 2.1: Map of Enclosure from Kerry's study of Adélie Penguins

This system was implemented and provided useful data. It was able to weigh, "on a colony basis, adult birds to an accuracy of ± 5%"; however, individual bird weights had an error of up to 10 to 15% [20].

Kerry et al. provides a brief description of calibration during the initial set-up, but continual calibration is not implemented [20]. Larios et al. provided a more comprehensive description of the technical requirements, advanced continual calibration and produced more accurate results using the neural network to estimate weights from unstable measurements [19] which is discssed in Section 2.6.2.

2.4.3 Predictive Models

In some studies, weight changes have been predicted based on other behavioural or physiological parameters. Lescroël et al. [21] built off the system developed by Kerry et al. [20] and demonstrated that foraging dive frequency could predict body mass gain in Adélie penguins. Time-depth recorders were attached to the penguins and recorded factors of the penguins' dive [21]. This was analysed with the weight that each penguin gained during the foraging trip (recorded from Kerry et al. [20] weighbridge) to determine which factors had the highest correlation with weight gain. The change in body mass of penguins at sea was largely explained by the number of foraging dives per hour and, to a lesser extent, the number of undulations per hour [21]. However, Lescroël et al. explain that the relationship between foraging behaviour and weight gain is highly species-specific and cannot be universally applied across all penguins or marine wildlife. This variability shows the necessity for species-specific validation of foraging success indicators and the importance of using multiple dive metrics when inferring foraging success from dive data [21]. Figure 2.2 shows the combined process with both the weighbridge and time-depth recorder.

2.4.4 Morphometric Indicators and Image Processing Methods

Another non-invasive approach involves using morphometric indicators to estimate body condition. Hayes and Shonkwiler [22] discussed how external measures like body mass, wing chord, and foot length are used to develop body condition indices. Two methods used to estimate body condition from external measurements involve creating ratio variables, such as by dividing body mass by length, and generating residual variables, such as residuals from the regression of mass on length [22]. While these

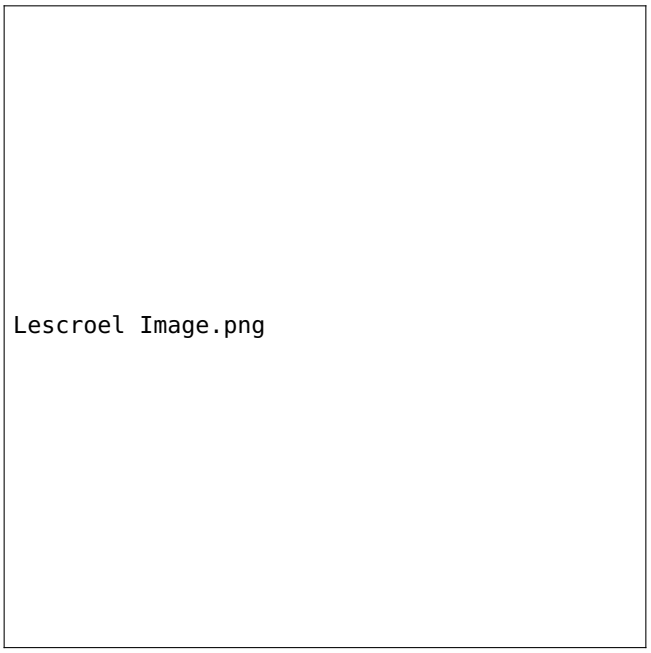

Figure 2.2: Predictive Weight Model through Foraging Process

indices don't directly measure weight, they provide valuable information about an animal's condition and can be obtained without direct handling. However, the accuracy of these indices in reflecting true weight or fat content can vary and requires careful interpretation [22]. Hayes and Shonkwiler advise that condition indices that are based on relationships between external morphological variables require external verification to be justified [22].

2.5 Non-invasive camera-based and sensor-based monitoring techniques

Non-invasive monitoring techniques play an important role in monitoring African Penguins to observe their behavioural patterns and gain insights into their moulting process. African penguins are highly suitable for visual detection since they have high contrast plumage patterns and stable markings. Penguins also have slow, predictable movements between breeding colonies and the sea making it easier to position camera systems [23] for image acquisition. This section focusses on various studies that have implemented cameras and sensors for wildlife tracking and the relevant challenges and similarities to African penguin monitoring techniques are discussed.

2.5.1 Remotely Operating Time lapsed Camera network

Southwell and Emmerson [24] implemented a remotely operating time-lapse camera system to track breeding activity of Adelie penguins found in Antarctica. The system included a digital single lens reflex camera housed within a weatherproof case and fitted with a transparent window for extra protection against snow and dust. Other important technology included a solar panel and a programmable camera controller. The lightweight, portable and easy to implement camera systems were deployed across four regions and were positioned to view the nests where they captured daily images of the full breeding season indicative of arrival timing, nest occupancy, egg-laying dates and chick presence and survival.

The data obtained strongly correlated with the direct estimates thus validating the system.

The cameras proved to be durable and had operated successfully for seven years at the time of the study. The authors estimate that a ten-year monitoring programme can be achieved at a tenth of a cost of a traditional monitoring programme. This system can be highly relevant for non-invasive monitoring of penguin colonies over longer periods. It is important to note that short-term moulting changes might be missed by when using a time lapse system and individual tracking can be difficult to implement.

2.5.2 Wireless Image sensor networks

A wildlife monitoring system developed by Zhang et al. [25] uses three pyroelectric infrared sensors to detect movement. Infrared LEDs and light sensors manage lighting, while two servos mounted on a stand orient the sensors in different directions. Animal movement in the detection zone triggers the system - the camera captures and compresses the images, which are tagged using the GPS for tracking. The system is specifically designed for *Cervus elaphus* in forested environments; however, it provides valuable architecture for non-invasive monitoring of African penguins during moult. The system operates using solar power and its event-based capturing ability that is programmed into the sink node makes it suitable for deployment in remote areas. However, the motion-triggered feature might not be suitable to penguins as they remain mostly stationary during moulting, but other system triggers can be investigated further.

2.5.3 Camera setup for weight measurement

The infrastructure implemented in the camera-based weight measurement system developed by Szabo and Alexy [26] offers key insights into real-world automated monitoring. IP66-rated security cameras which are weather, and dust proof were utilised in this study. The camera and scale were fixed to the metal-based roof structure of the barn. The study encountered a similar challenge to African penguin monitoring which is individual tracking and encouraging the birds to step on the scale. The images taken by the camera were further processed by machine learning techniques discussed as discussed in Section 2.6.3

2.5.4 Monitoring using an Unmanned aircraft system (UAS)

Aerial imaging technology such as the camera-equipped light unmanned aircraft system implemented by Sarda-Palomera et al. [27] presents an effective, non-invasive method to obtain real-time data with minimal intervention. The system was tested on a dense colony of Black-headed Gulls and consisted of an electric-powered, manually controlled aerial platform, equipped with a downward facing camera and a GPS for tracking. The total weight of the system was 2.0kg and the cost of the model was €1400.

The system was hand-launched and had no under carriage therefore allowing it to land on small, flat areas. Images were captured through two daily flights, with high-resolution photographs used to identify individual gulls and assess colony structure. The camera operated in continuous shooting mode, enabling full-colony coverage during each flight. The images were subsequently processed and validated, and the the system to accurately estimated the number of nests in the colony. This study validates the use of simple drone-mounted cameras for non-invasive monitoring as it can completely

remove ground disturbance. The challenge of this implementation, however, is the rocky terrain of African Penguins, the management of battery life and weather tolerance for a coastal environment.

2.6 Machine Learning Applications in Avian Health and Identification

Machine learning (closely related to artificial intelligence) is a relatively new concept; however, in the short time it has been around, it has completely reshaped wildlife monitoring systems. Monitoring birdlife – especially the African penguin – is no exception. The following section explores how machine learning can be used in the conservation of the African penguin.

2.6.1 Machine Learning and Species Distribution Models

Geldenhuys developed species distribution models (SDMs) using the MaxEnt algorithm. This allowed her to map suitable habitats for African penguin colonies. She was able to model seasonal and annual habitat suitability across southern Africa using data from 33 colonies. Geldehuys' research identified key drivers of habitat suitability and sustainability: sea surface temperature (the primary contributor) and mean land temperature (the secondary contributor). Using these key drivers, she was able to propose two potential new colony sites: De Hoop and Plettenberg Bay [28].

The study has various strengths and weaknesses. Some of its key strengths include robust use of machine learning for ecological forecasting and the establishment of a clear link between environmental data and conservation planning. However, it has its limitations: it relied on presence-only data meaning it did not include information about where African penguins are not present [28].

2.6.2 Artificial Neural Networks (ANN) for Weight Estimation

An Artificial Neural Network (ANN)is a type ofmachine learning modelinspired by how thehuman brainprocesses information [29]. Larios et al. used ANNs to monitor wild animal body mass. Sensors on weighing platforms captured unstable readings due to animal motion and the ANN was trained to distinguish between valid weight readings and artefacts caused by movement. This is a non-invasive (no direct handling required) automatic weighing system [19].

The ANN approach can effectively filter real vs. false signals. It is applicable to wild species where non-invasive data collection is critical. However, the researchers did not test the technology specifically on African penguins.

2.6.3 Image Processing and Machine Learning for Weight Estimation

Szabó and Alexy combined image processing with Random Forest regression to estimate duck body mass in a commercial farming setting. Photos were taken of the ducks when they stood on the scale and their weights were simultaneously recorded. The researchers were able to train the model using the image-weight pairs. After the model was trained, it could estimate duck body mass simply through image processing [26].

The model demonstrated high accuracy and is a non-invasive, camera-based system; however, its accuracy was dependent on the environment. It worked best in the specific barn environment where it was trained – the model cannot be generalised [26]. Furthermore, the study focused on ducks. Species-specific training would be required to apply the model to penguins. This shows that since Hayes and Shonkwiler discussed metamorphic indices (discussed in Section 2.4.4), the development in technology has allowed for more accurate weight estimation based on visual information [22].

2.6.4 Computer Vision for Individual Identification Using Machine Learning

Sherley et al. developed a computer vision biometric system to identify African penguins in a controlled environment using their unique chest spot patterns. A machine learning model was trained on videos of penguins moving along a predictable route on Robben Island. The algorithm could then match individuals against a biometric image database with incredible accuracy. The researchers avoided the use of flipper bands allowing for long-term identification without physical tagging [23].

This study is promising: the researchers' method is non-invasive and highly accurate. The model was able to correctly identify a penguin 96.7% of the time [23]. Some of the limitations of the study include: the accuracy of the algorithm is dependent on penguin movement patterns. It worked best when the penguins passed the camera one at a time – allowing a clear view of their chest spot patterns. Therefore, this method may be less effective in less structured colony settings.

2.7 Conclusion

The literature reviewed demonstrates the significant physiological changes African Penguins undergo during moulting and the range of factors that can disrupt this process. Effective monitoring is essential for conservation, but traditional invasive methods can exacerbate stress. The studies reviewed highlight the potential of non-invasive methods, including technological advancements and machine learning applications, for monitoring penguin health. These methods offer promising avenues for future research and conservation efforts, enabling more accurate and less disruptive data collection. Therefore, the development and implementation of non-invasive techniques, such as automated weighing systems and image-based analysis, are crucial for the future of African Penguin research and conservation.

Chapter 3

Chassis Body and Scraper Subsystem

3.1 Introduction

The design, development, and validation of the Chassis and Scraper Subsystem is thoroughly outlined in this section of the report. The subsystem provides support for the structural and dynamic components of the overall system. The chassis features dedicated cavities to house the servo motors and a sealed compartment to protect the system's electrical components. The sealed compartment has a removable lid for easy access and maintenance. The subsystem is also equipped with a front-facing camera mount and a mechanised scraper blade to collect faecal samples. The mechanised scraper blade includes two levers actuated by separate servo motors. All of the parts discussed in this section were designed using Autodesk Inventor and 3D-printed using PLA filament. This ensures that they integrate seamlessly with the base of the tank-track and perform well in the field.

3.2 Requirement Analysis

3.2.1 Traceability Matrix

The table below shows how each user requirement was converted to practical design goals, measurable specifications, and validated through acceptance testing procedures to ensure all parts function as expected.

User Req.	**Functional Req.**	**Specification**	**ATP**
UR01 Remote Operation for Sample Collection	FR1	S1	ATP1
UR02 Visual Monitoring Capability	FR3	S5	ATP5
UR04 Sample Collection Mechanism	FR1	S1	ATP1
UR05 Sample Storage	FR1	—	—
UR06 Robustness for the Environment	FR5, FR11	S7, S12	ATP7, ATP13
UR07 Ease of Use for Ornithologists	FR9	S4	ATP4
UR08 Budgetary Constraints	FR7	S10	ATP10

Table 3.1: Traceability Matrix for the Chassis and Scraper Subsystem

3.2.2 Functional Requirements

Requirement ID	Description
FR1	The subsystem must include a motorised scraper blade to perform surface-level sample collection.
FR2	The chassis must contain a sealed compartment to securely enclose all electronic components.
FR3	A forward-mounted camera must be included to enable remote navigation and monitoring.
FR4	All components must be designed using CAD software and fabricated using FDM 3D printing.
FR5	The printed structure must be mechanically robust and resist failure under typical field stresses.
FR6	The chassis must fit on the tank-track platform without interfering with its motion.
FR7	The subsystem must be cost-effective and constructed using affordable, readily available materials such as PLA.
FR8	All components must be easy to assemble using adhesives or ISO standard fasteners.
FR9	The electronics enclosure must feature a removable lid to allow easy access during assembly and maintenance.
FR10	The subsystem must visually blend with the environment to avoid disturbing penguins.
FR11	The subsystem must be water-resistant to protect internal components from environmental exposure.

Table 3.2: Functional Requirements for the Chassis and Scraper Subsystem

3.2.3 Specifications

Spec ID	Specification	Related FR
S1	The scraper arms, driven by two MG90S servo motors, must rotate through at least 90° to ensure full actuation.	FR1
S2	The chassis must contain two servo cavities, each measuring 23 mm × 12 mm × 24 mm with at least 0.25 mm clearance on all sides.	FR1, FR2
S3	The sealed compartment must accommodate a motor driver, two voltage regulators, a connection hub, and a battery with maximum 3 mm clearance. Dimensions: 88 mm x 60 mm x 60 mm.	FR2, FR9
S4	The compartment lid must be removable without the use of tools — for example, via a sliding slot mechanism.	FR9
S5	The ESP32-CAM must be mounted on a front-facing bracket angled at approximately 20° from vertical.	FR3
S6	All components must be printable using 1.75 mm PLA filament on a standard desktop FDM printer such as the Creality Ender 3V2.	FR4, FR7
S7	The minimum wall thickness of structural elements must be between 1.2 mm and 1.6 mm to ensure mechanical stability.	FR5
S8	The assembled subsystem must fit within a 140 mm × 75 mm footprint and not exceed 100 mm in height.	FR6
S9	At least 10 mm clearance must be maintained between the chassis and the tank tracks.	FR6
S10	The total material cost must not exceed R500.	FR7
S11	The chassis exterior must be matte black or coated in a similarly low-visibility tone to visually blend into natural environments.	FR10
S12	All seams, openings, and lid interfaces must be sealed or designed to resist water ingress under light spray conditions.	FR11

Table 3.3: Subsystem Specifications

3.2.4 Acceptance Test Procedures (ATPs)

The following procedures define how each subsystem specification will be verified. Each test includes a method and a measurable acceptance criterion.

ATP ID	Test Description	Acceptance Criteria
ATP1	Rotate the scraper arms manually and via PWM input. Measure rotation angle with a protractor.	Each arm rotates at least 90° without mechanical interference.
ATP2	Insert MG90S servos into their cavities and check fit manually.	Servos insert easily, sit firmly, and align with the output shaft slot.
ATP3	Fit the motor driver, regulators, hub, and battery into the sealed compartment.	All components fit with ≤ 3 mm clearance and no contact with the lid.
ATP4	Remove and reseat the lid 3 times without tools.	Lid attaches and detaches cleanly with no deformation or misalignment.
ATP5	Mount the ESP32-CAM and verify alignment using a live video feed.	Camera is securely mounted and has clear, unobstructed forward view.
ATP6	Print all components using 1.75 mm PLA on a Creality Ender 3V2.	All parts print successfully with no slicing errors or print failures.
ATP7	Apply thumb pressure to structural features and mounting points.	No visible deformation, cracking, or flex observed.
ATP8	Measure the subsystem's dimensions with calipers.	Dimensions do not exceed 140 mm $\times$ 75 mm $\times$ 100 mm.
ATP9	Mount chassis on tank base and rotate arms. Measure track clearance.	No collisions; minimum 10 mm clearance is maintained.
ATP10	Calculate filament cost from slicer data and compare to actual spend.	Total material cost is $\leq$ R500.
ATP11	Visually inspect the final assembly for a matte black or low-contrast surface finish.	Exterior finish must be non-reflective and visually neutral in outdoor settings.
ATP12	Perform a light water spray test over the chassis with electronics installed.	No moisture present inside the electronics compartment after test.

Table 3.4: Acceptance Test Procedures (ATPs) for the Chassis and Scraper Subsystem

3.3 Design Choices

This section discusses key design decisions made during the development of the Chassis and Scraper Subsystem. For each decision, multiple alternatives were considered and evaluated based on cost, reliability, ease of implementation, and subsystem constraints.

3.3.1 Scraper Actuation Method

Option A: Dual servo-actuated lever arms (final choice)
Two MG90S servo motors are housed at the front of the subsystem. Each motor drives a rigid arm directly connected to the scraper blade, enabling a smooth and controlled sweeping motion. This approach allows precise angular displacement and coordinated actuation of the scraper. It is simple, compact, and technically mature, with well-documented servo control via PWM signals.

Option B: Rack-and-pinion with a single motor
An alternative considered was a rack-and-pinion system, where a single motor drives a linear rack to push or pull the scraper blade. While potentially reducing the number of motors, this method adds complexity in terms of gear alignment, increases mechanical parts, and requires more technical precision. It also complicates 3D printing and testing.

3.3.2 Camera Mount Integration

Option A: Fixed front-facing external mount (final choice)
The final design includes a rigid, angled bracket mounted externally at the front of the chassis to hold the ESP32-CAM. This setup offers an unobstructed forward view and avoids placing the camera inside the sealed enclosure. It simplifies wiring, speeds up installation, and reduces print complexity. Importantly, the external positioning of the ESP32-CAM also enables easier disconnection and reprogramming, which is highly beneficial during field debugging and testing.

Option B: Internal tilting camera mount
An internal tilting mount was also considered, where the camera would sit behind a transparent window and be angled via an additional MG90S servo. Although this would allow dynamic view adjustment, it increases the number of components, consumes space inside the electronics compartment, and makes waterproofing more difficult. The added complexity and limited advantage in this application led to its rejection.

3.3.3 Mounting and Assembly Material

Option A: Prestik (final choice)
Prestik was chosen as the preferred mounting and temporary fastening solution for lightweight, non-load-bearing components. It allows for fast, reversible attachment and aligns well with the modularity goal of the subsystem. It supports easy removal, prototyping, and maintenance without introducing residue or permanent bonds.

Option B: Super glue (cyanoacrylate)
Super glue was initially considered for bonding lightweight components such as the camera bracket. However, it forms a permanent bond and complicates rework or reassembly. While it provides higher shear strength, it reduces modularity and is more prone to accidental damage during upgrades or maintenance. Therefore, Prestik was chosen to enhance system modularity and ease of testing.

3.3.4 Design Choice Comparison

The following table compares the two options considered for each design decision, evaluated across several figures of merit.

Figure of Merit	**Dual Servo Lever Arm (Chosen)**	**Rack-and-Pinion Mechanism**
Cost	Low – two MG90S servos are inexpensive and widely available	Moderate – requires additional gears, rods, and precision parts
Technical Maturity	High – standard micro servo use is well documented	Moderate – less common in small-scale, low-load applications
Ease of Manufacturing	High – directly printable components, minimal post-processing	Low – requires accurate gear meshing and tight tolerances
Ease of Implementation	High – simple PWM control and mechanical layout	Low – more complex control and mounting geometry
Ease of Testing	High – direct actuation and observable motion make testing easy	Moderate – motion depends on multiple interacting parts
Reliability	Moderate–High – limited parts, but exposed joints	Moderate – more moving parts, risk of mechanical backlash
Maintenance Cost	Low – easily replaceable servos	Moderate – gear systems may wear and require realignment

Table 3.5: Comparison of Scraper Actuation Design Options

Figure of Merit	**External Fixed Mount (Chosen)**	**Internal Tilting Mount**
Cost	Low – minimal extra material and no additional servo	Moderate – adds a third servo and support structure
Technical Maturity	High – fixed camera mounting is standard and reliable	Moderate – internal tilt systems are less common in small mobile platforms
Ease of Manufacturing	High – single-piece print or bracket mount	Low – requires precision assembly of internal mount and pivot
Ease of Implementation	High – straightforward wiring and positioning	Low – adds extra servo control and rotation limits
Ease of Testing	High – static view simplifies camera alignment tests	Moderate – tilt system adds calibration steps
Reliability	High – no moving parts in mount	Moderate – tilt mechanism introduces wear points and failure risk
Maintenance Cost	Low – easily accessed and replaceable camera	Moderate – internal access may require partial disassembly

Table 3.6: Comparison of Camera Mount Design Options

3.3.5 Deciding Which Track-tank to Use

The track-tank was selected due to its versatility and modularity. Its base includes multiple unused mounting holes, which allow for relatively easy attachment of custom components. Furthermore, the open structure of the base provides convenient routing paths for wiring, simplifying the integration of electrical components without obstructing mobility or access.

3.4 Submodule Design

3.4.1 CAD Modelling and Final Design

Autodesk Inventor was used to model all submodules. The submodules were designed for 3D printing with 1.75 mm PLA filament on a Creality Ender printer. Black PLA was specifically chosen to help the subsystem visually blend into the environment and avoid disturbing penguins. All components were printed with 40% infill to maximise durability while maintaining a balance between print time and material usage. Supports were enabled for all prints to prevent deformation during overhangs and ensure dimensional accuracy. The subsystem consists of the following submodules: a main chassis body with a removable lid for accessing the internal components, two mechanised scraper arms that are rigidly connected to a scraper blade, and a front-facing ESP32-CAM mount.

Important dimensions relating to each submodule are illustrated in figure 3.1 to 3.6.

3.4.2 Chassis Body

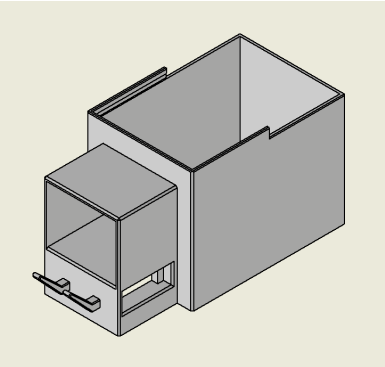

Figure 3.1: Chassis Body

Servo Motor Housing

The chassis features two rectangular cavities located near the front of its body that are designed to secure the servo motors in place. The cavities have a 0.35 mm clearance on either side and a 0.25 mm clearance on the top and bottom providing a snug fit.

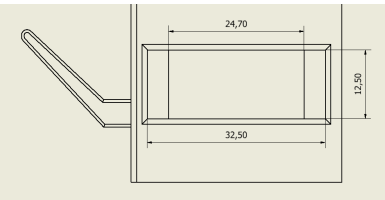

Figure 3.2: Front View

Electrical Components Compartment

The chassis contains an enclosure designed to house a motor driver, two voltage regulators, a connection hub, and a battery. Its walls are 2 mm in thickness - balancing durability with print time and material

usage - and are fitted with a 0.8 mm sliding slot. The chassis includes integrated pathways between the servo motor housings and the electrical components enclosure to accommodate internal wiring.

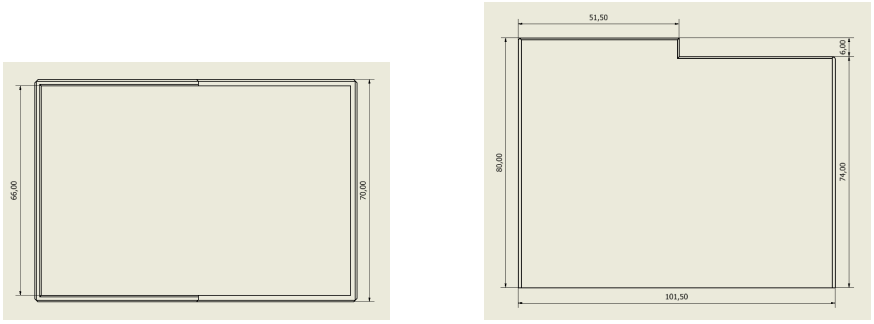

(a) Top View (b) Side View

Figure 3.3: Electrical Components Compartment

Removable Lid

The enclosure is sealed by a removable lid held in place via a sliding slot. This provides easy access to the electrical components, simplifying maintenance and eliminating the need to disassemble the chassis. To conserve filament and reduce waste, the lid was fabricated from reused plastic — specifically, cut from an old ice cream tub. It was painted matte black to blend with the natural environment and minimise visual disturbance.

3.4.3 Scraper Blade

The scraper blade spans the front of the chassis and is rigidly secured between the two mechanised arms. Its slanted edge is sharp and angled slightly downward to enhance scraping performance. As discussed previously, the scraper arms are rigidly attached to the scraper blade; therefore, ISO standard M3 tapped holes are made on either side of the scraper blade. The scraper blade was designed using minimal material while still maintaining its ability to collect and hold faecal samples to limit print time and material usage.

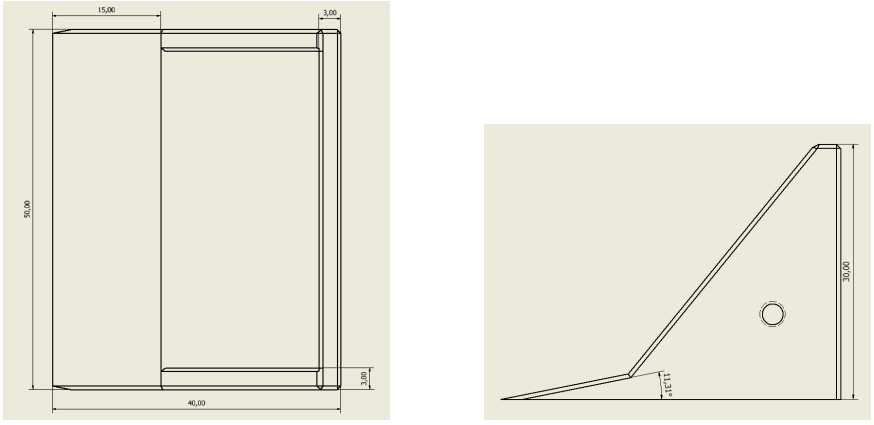

(a) Top View (b) Side View

Figure 3.4: Scraper Blade

3.4.4 Scraper Arms

The scraper arms are rigid levers actuated directly by MG90S servo motors. Each arm is 80 mm long and has a thickness of 5 mm to improve mechanical performance under load. A built-in negative geometry interfaces with the servo horn, enabling a direct press-fit connection. This approach was intentionally selected to eliminate the need for adhesives or additional fasteners, simplifying assembly and allowing for easy disassembly during testing. Finally, an ISO standard M3 clearance hole is made at the end of each arm, where an 18 mm fastener is used to rigidly attach the scraper arms to the scraper blade.

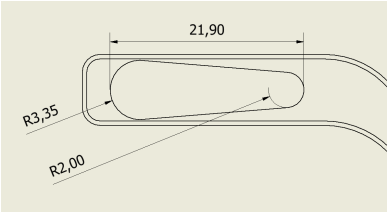

Figure 3.5: Negative Geometry

3.4.5 Camera Mount

The ESP32-CAM is attached to a fixed mounting bracket using Prestik. The bracket is located on the front face of the chassis and makes a ≈20° angle with the vertical. The camera is therefore directed towards the ground. It is imperative that the camera has a clear view of the surface since this is ultimately where the faecal matter will be located. The bracket is 3 mm thick at its thinnest point allowing

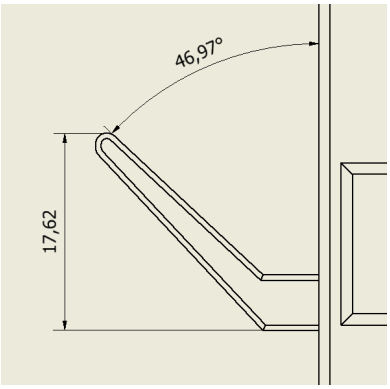

Figure 3.6: Camera Mount

3.4.6 Scraper Arms Motion Simulation

A study was conducted in Autodesk Inventor to verify that the mechanised arms achieved the desired 90° range of motion. Figure 3.7a, 3.7b and 3.7c illustrate the scraper arms in three distinct positions: 0°, 90°, and 180°. It is clear that the mechanised arms are unobstructed and have a full 180° range of motion - exceeding the required 90° outlined in 3.2.3.

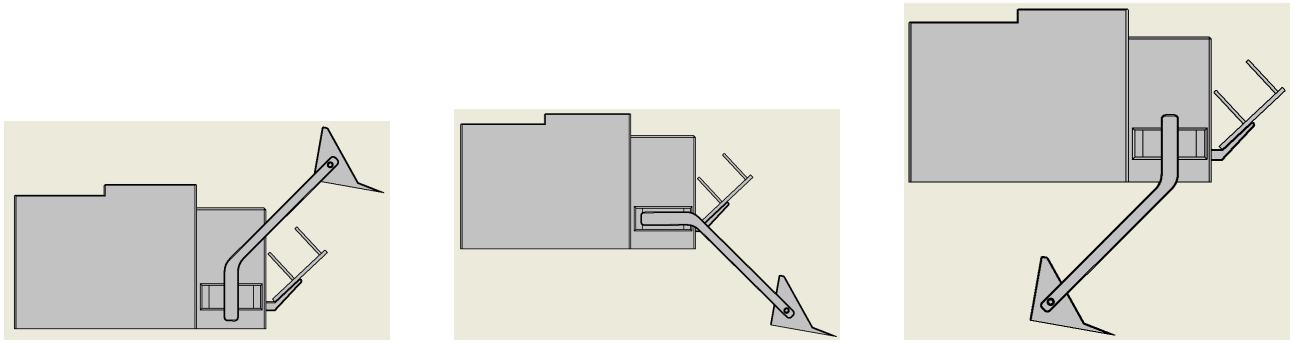

(a) 0° (b) 90° (c) 180°

Figure 3.7: Scraper Arms Range of Motion

3.4.7 Cost Calculation

Component	Mass (g)	Filament Used (m)	Price/gram (R)	Total Cost (R)
Chassis Body and Camera Mount	82.37	32.93	0.45	R37.07
Scraper Arms (×2)	4.67	1.87	0.45	R2.10
Scraper Blade	7.63	3.05	0.45	R3.43
Total	94.67	—	—	**R42.60**

Table 3.7: Estimated PLA material cost for all 3D printed components

3.5 ATP Results Summary

ATP ID	Test Description	Result	Remarks
ATP1	Scraper arm range of motion	Passed	180° range of motion achieved
ATP2	Servo cavity fit	Passed	MG90S servo motors fit tightly inside cavities
ATP3	Internal component fit	Passed	Electrical components fit with ≤ 3 mm clearance
ATP4	Lid removal and reseating	Passed	Lid removed/reseated cleanly 3 times with no issues
ATP5	ESP32-CAM mounting	Passed	Camera mounted securely; unobstructed view confirmed
ATP6	3D print feasibility (FDM)	Passed	All parts printed cleanly with 1.75 mm PLA on Ender 3V2
ATP7	Manual stress test	Passed	No visible deformation or cracking under applied pressure
ATP8	Final dimensions check	Passed	Actual: 140 mm × 70 mm × 80 mm
ATP9	Track clearance verification	Passed	Minimum 10 mm clearance achieved; no contact
ATP10	Material cost check	Passed	Total material cost within budget ($\leq$ R500)
ATP11	Post-processing inspection	Passed	No major support issues; only basic removal required
ATP12	Matte black environmental blending check	Passed	Entire subsystem finished in matte black
ATP13	Waterproofing (spray test)	Not Passed	Minor water ingress observed; further sealing required

Table 3.8: Acceptance Test Procedure Results for Chassis and Scraper Subsystem

3.6 Design Refinements and Optimisations

Following ATP testing and several development iterations, a range of mechanical and manufacturing refinements and optimisations were introduced to enhance the subsystem's efficiency. One of the significant changes involved reducing the thickness of all non-load bearing walls from 3 mm to 2 mm. This seemingly minor adjustment dramatically cut down on filament usage and reduced printing time from roughly 16 hours to 13 hours, without compromising durability. Furthermore, excess material was also strategically removed to improve efficiency and printing speed.

Another major improvement was combining separate parts, like the camera mount and chassis body, into a single unified print. This removed the need for glue or manual alignment, made the overall structure sturdier at the mount, and allowed uninterrupted overnight printing with minimal supervision.

In response to a failed waterproofing test, a potential improvement was identified: adding a small protective roof above the camera bracket to shield it from water exposure. This would reduce the risk of moisture ingress through the camera interface while minimally impacting print complexity or footprint.

Zipties were also considered as a potential replacement for Prestik to secure the chassis to the tank-track platform. By feeding zipties through existing holes in the base plate, a much more stable and durable connection could be achieved — while still allowing for modular disassembly if needed.

Several additional refinements were considered for future iterations. These include adding chamfers or fillets to sharp edges to reduce stress points and improve print reliability, as well as incorporating internal clips or guides for cleaner cable management.

Overall, the adjustments made throughout the design process significantly improved the subsystem's efficiency, durability, and ease of manufacturing, without compromising any of the user requirements.

3.7 Conclusion

The final Chassis and Scraper Subsystem met all the user and functional requirements through a process of design, development, testing, and refinement. It successfully enabled reliable, non-invasive faecal sample collection using a dual servo scraper, while securely housing the electrical components and providing a stable mount for the front-facing camera. Each design decision was guided by thorough comparisons and was validated through CAD simulations, physical prototyping, and rigorous testing. The result is a compact, robust and budget-friendly solution that integrates seamlessly into a larger robotic system.

Chapter 4

Electrical Subsystem and Locomotion

Prepared by: Rachael Guise-Brown (GSBRAC001)

4.1 Introduction

This subsystem focuses on the electrical components and their integration with the mechanical systems and processor, required for the system to manoeuvre and collect faecal matter. It encompasses the selection of the components necessary providing the electrical signals and power required for the vehicle's locomotion and the operation of the scooping mechanism and ensures reliable electrical connections through the system.

4.2 Requirements

The subsystem requires the following components to meet the user requirements specific for this subsystem:

- **UR01 and UR06:** Wheels or tracks with motors for locomotion for robust, remote operation in the penguin environment.
- **UR03:** Power source for wireless operation.
- **UR04:** Connections required for motors for scooping.

The functional requirements and specifications for each required component is detailed in Tables 5.1 and 5.2 respectively in relation to the user requirements. The acceptance tests for the specifications are detailed in Table 4.10 in Section 4.5. Additionally, based on the decision from the other two subsystems - the processor that needs to be supported is a ESP32-CAM and the motors used for scooping are two FS90R 180 degree servo motors.

4.3 Design Choices

The interconnected nature of the electrical components means that the design choice of one item can significantly affect the compatibility and performance of others. To manage these inter dependencies, the components were selected in the following order:

1. **Wheels/Tracks:** Chosen based on system weight to ensure stability and traction on uneven terrain.

Table 4.1: Functional Requirements

UR ID	**FR ID**	**Functional Requirement**
UR01	FR01	Motors must connect to the processor and interface with wheels/tracks for locomotion.
UR06	FR02	Motors must provide sufficient torque to move the system across uneven terrain.
UR06	FR03	Wheels/tracks must support the full weight of the system.
UR01	FR04	Wheels/tracks must be actuated by the motors.
UR06	FR05	Wheels/tracks must provide stability and traction on uneven terrain.
UR06	FR06	Wheels/tracks must ensure smooth and steady movement.
UR01, UR03	FR07	Power source must supply adequate voltage and current to all electrical components.
UR01, UR03	FR08	Power source must sustain operation long enough for a full deployment to allow collection of faecal matter.
UR01	FR09	Power source must be disconnect-able for safety and maintenance.
UR01	FR10	All electrical components must be interconnected reliably.

Table 4.2: Specifications Linked to Functional and User Requirements

Spec ID	**Specification**	**Linked FR(s)**	**ATP ID**
SP01	Motors must provide a minimum torque of **0.3 Nm** to be able to handle the weight and uneven terrain.	FR02	ATP01
SP02	Wheels/tracks must support at least **5 kg** system weight.	FR03	ATP02
SP03	Wheels/tracks must handle inclines of **15°** and obstacles up to **2 cm**.	FR05	ATP03
SP04	Motors must respond to PWM control with a latency under **half a second**.	FR01, FR04	ATP04
SP05	Power supply must be able to deliver at least **5V** for the processor and the voltage required for the motors (dependant on the motor choice).	FR07	ATP05
SP06	Power supply must be able to deliver **continuous and peak current** required by the whole system (processor and motors) under full load.	FR07	ATP06
SP07	System must operate continuously for at least **1 hour**.	FR08	ATP07
SP08	Include a **manual disconnection switch** for power safety.	FR09	ATP08
SP09	Use secure, standard connectors for all electrical links.	FR10	ATP09
SP10	All motor mounting fasteners must be mechanically secured	FR01, FR04	ATP10
SP11	Locomotion system's speed must be in the range **0.1m/s - 0.3m/s** at full speed on flat terrain.	FR02, FR06	ATP11

2. **Motors:** Selected to provide sufficient torque for the system and drive the chosen wheels.
    (a) Motor driver: Potentially required for interfacing motors with the processor.
3. **Power Source:** Must supply adequate voltage and current for the processor, motors, and drivers.
    (a) Voltage Regulators: Used to maintain stable, component-safe voltage levels.

The following subsections detail the specific design choices made for each component.

4.3.1 Wheels or Tracks

The selection of wheels or tracks is crucial for the vehicle, as they directly impact its ability to traverse the uneven terrain it will encounter (SP02, SP03, SP11). The wheels or tracks must provide adequate traction and stability to ensure smooth and steady movement, while supporting the weight of the entire system.

There many available wheels at reasonable prices, therefore, these were considered first. A comparison of wheel options considered in the design process is presented in Table 4.3:

Table 4.3: Wheel Comparison

Feature	**42mm Wheel**	**65mm Wheel**	**60mm Silicone Tyres**
Wheel Type	Thick rubber tyre with deep tread	Thin rubber tyre with light tread	Silicone tyre with horizontal tread
Wheel Measurements	42 mm diameter × 19 mm width	65 mm diameter	60 mm diameter × 8 mm width
Traction (based on wheel tread and material)	Moderate	Moderate	Low
Cost (wheel + motor)	R75.75	R41.29	R158.70 (for two)

The 65mm thin rubber tyre offered a good balance of tractionand cost-effectiveness. However, the ESP32-CAM's limited GPIO pins restrict direct control of more than two motors and, therefore, no more than two wheels can be independently controlled. Two wheels provide limited stability for the whole system (SP03) and without including additional port expanders or processor to be able to control more motors, increasing the stability is not possible. This led to tank tracks being considered instead of wheels.

Tank tracks were chosen for their superior stability, traction, and weight distribution on uneven terrain using only two motors (SP03, SP02). These qualities are critical for navigating the penguin enclosure and transporting samples reliably. However, very few suitable tank tracks were available in South Africa from approved suppliers within budget. 3D printing was considered to address this, but available materials lacked the strength and durability needed for rough terrain, and stronger options (like TPU or reinforced nylon) were not accessible. As a result, a pre-manufactured tank track set was selected for its robustness, reliability, and ease of integration. The tracks, drive wheels, and bearing wheels are shown in Section 4.4, Figure 4.2.

4.3.2 Motors

The motors are responsible for providing the torque and speed necessary to propel the vehicle and support its load, including the scooper, processor, camera, and batteries (SP01, SP10). Their selection must ensure compatibility with the chosen tracks and sufficient torque for movement on uneven terrain and inclines (SP01, SP03).

Table ?? presents a comparison of the motors considered:

The *F-MINGNIAN-TOOL GB-520 DC Gear Motor* was selected due to its superior torque, robust

Characteristic	N20 Micro Gear Motor	TT Gear Motor	FSR90 Servo (Continuous)	F-MINGNIAN-TOOL GB-520 DC Gear Motor
Rated Voltage	6V	3–6V	5V	6–12V
Speed (RPM)	∼300	∼200	∼100	170–350
Torque	0.35kg/cm	0.8kg/cm	1.5kg/cm	5kg/cm
Key Features	Compact size, widely available	Inexpensive, easy to mount	Easy control using PWM, lightweight	All-metal gearbox, 5mm shaft, suitable for high-load systems

Table 4.4: Comparison of motor options considered for the drive system.

all-metal gearbox, and appropriate speed range for the tank drive system. Its 5 mm shaft diameter fits the track hubs, and it can reliably handle the loads expected in operation. The N20 and TT motors were insufficient in torque, while the FSR90 servo, though easy to control, lacked the mechanical robustness required. It is shown in Figure 4.2.

Motor Driver

The F-MINGNIAN-TOOL GB-520 DC gear motors require a motor driver, as microcontrollers operate at low voltages (3.3V) and cannot supply sufficient current. Motor drivers amplify these low-power signals to drive the motors effectively.

An integrated motor driver IC was selected over a custom circuit for its built-in protection, efficient switching, and compact design. A module version of the IC was chosen for its comparable cost (UR08), enhanced reliability from manufacturer testing, and ease of integration via pin headers and onboard passive components (SR09).

Based on the specifications of the chosen motor and processor, the following key motor driver requirements were identified:

- Input voltage: 3.3V, to match the processor's GPIO output levels and compatible with PWM for speed control,
- Output voltage capability: 6V to 12V, to match the motor's rated voltage,
- Output current capacity: at least 0.5–1A per channel, to allow for motor stall conditions despite a no-load current of 100mA.

The L298N Mini motor driver was chosen for its balance of features and cost-effectiveness. The standard L298N is unsuitable because its control signal requirements are not compatible with the ESP32-CAM's output voltage. The TB6612FNG is more efficient but also more expensive (UR08). The L298N Mini, while handling a lower maximum voltage, is compatible with the motors, provides sufficient current capacity, PWM support, and thermal shutdown protection, all in a compact and affordable package.

4.3.3 Power Source

To enable autonomous operation, the vehicle uses a simple on-board power source without charging or battery monitoring (SP05, SP06, SP07). It must deliver up to 9V to the motors via the motor driver

Table 4.5: Motor Driver Comparison

Feature	**MX1616 (L298N Mini)**	**L298N**	**TB6612FNG**
Channels (number of motors controlled)	2	2	2
Voltage Range (Motor)	2 V to 10 V	5 V to 35 V	4.5 V to 13.5 V
Current Capacity (Continuous)	1.5 A	2 A	1.2 A
Current Capacity (Peak)	2 A (with heat sink)	3 A	2 A
Control Signal (all support PWM)	1.8 V to 7 V	5 V to 12 V	2.7 V to 5.5 V
Cost	R28.75	R44.85	R176
Other Features	Compact Size	Widely Available	High Efficiency

(rated for 6–12V operation fro the motors, max 10V input for the motor driver) and a regulated 5V supply for the processor, which further steps down to 3.3V for logic operations within the processor board.

Selection was guided by simplicity (SP09), cost-effectiveness (UR08), and low weight for improved balance and agility (SP02).

Battery types with low energy density—like NiMH, SLA, and Alkaline—were excluded. The options compared are shown in Table 4.6.

Table 4.6: Battery Type Comparison

Battery Type	**Voltage (V)**	**Pros**	**Cons**
Lithium Iron Phosphate (LiFePO4)	3.2 per cell	Safer than other lithium chemistries, long cycle life, stable discharge voltage	Higher cost, lower energy density than other Li-ion
Lithium Polymer (LiPo) / Lithium-ion (Li-ion)	3.7 nominal	Very high energy density, lightweight	Requires careful handling
USB Power Bank	5	Convenient, integrated protection, readily available	Designed for low current draw, adds weight of circuitry, may not be suitable for high-power motors

Voltage regulation is essential to maintain stable output as the battery discharges. Options for meeting the 5V and 9V requirements are compared in Table 4.7.

The most suitable option was the high-voltage source regulated down for each component. This enables near-optimal motor performance with 9V output, while a separate regulator provides 5V to the processor. Despite the added complexity, this setup balances performance, reliability, and component availability. Intermediate voltage sources were rejected due to poor motor performance and heat losses at the processor, while low-voltage sources with boost converters introduced inefficiency and noise.

The final design uses 18650 lithium-ion cells, chosen for their high energy density, compactness, and affordability (SP02, UR08). A 3S configuration (three cells in series) delivers 11.1V nominal (range: 9V–12.6V). This regulated for:

Table 4.7: Power Source Options

Option	Regulators	Pros	Cons
6–7V Source Meets both components' ranges.	1 regulator (6–7V)	Simple design, fewer components.	Motors underpowered; processor dissipates excess voltage as heat.
5V Source + Boost 5V battery for processor, boosted for motors.	1 regulator, 1 boost converter	Lightweight battery; efficient processor supply.	Requires boost converter; adds noise and complexity.
High Voltage + Step-Down High-voltage battery regulated down for both.	2 regulators	Many battery/regulator options.	More components; heavier and less efficient.

- **Motor Supply:** Regulated to 9V for consistent motor performance (SR11).
- **Processor Supply:** Regulated to 5V for stable logic operations (SR03).

Voltage Regulator

Both voltage regulators must accommodate the full range of the 3S battery configuration, i.e., an input voltage between 9V and 12.6V. Two regulators are required—one for the motors and one for the processor—each with different voltage and current output needs, as outlined below.

- **Motor Voltage Regulator:** Must produce a stable output of 9V to power the motors. Given a no-load current of 100mA per motor, the regulator should be rated for at least 1A to account for increased current during loaded operation and startup surges.
- **Processor Voltage Regulator:** Must provide a constant 5V output, with a maximum current draw of 600mA based on processor specifications.

Due to the potential for high peak current—particularly in motor stall conditions—and the need for efficiency, switching regulators (buck converters) were selected instead of linear regulators. Linear regulators such as the L7805 and LM317T, while simple and low-cost, are not well-suited for high current applications due to excessive heat dissipation and limited current capacity. In contrast, buck converters offer higher efficiency and can support larger current loads with reduced thermal concerns.

The chosen buck converter is based on the XL4015 chip. It supports an adjustable output voltage range of 1.25V to 32V and is capable of delivering up to 5A of current, making it ideal for both the processor's 5V supply and the motor's 9–12V supply. Two of these regulators are used: one configured for the 5V processor rail and another for the motor rail. This solution is also cost-effective, with each module priced at only R38.00, and readily available in local stock.

4.4 Sub-Module Design

A summary of all the electrical components and their interfacing is shown in Figure 4.1.

4.4.1 Compiling Individual Components

Some of the components needed to be individually built, adapted or tested for integration with the whole system.

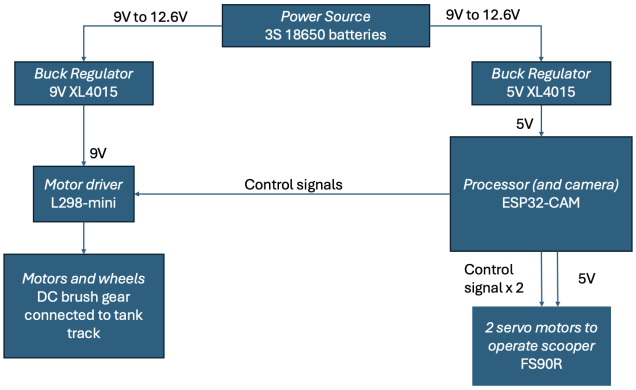

Figure 4.1: Interfacing of components

Motors and Tank Tracks.

The motors and tank tracks were assembled and attached to the chassis using bolts and nuts to keep it secure (SP10). The individual components and final assembly is shown in Figure 4.2. The tank track length was adjustable by removing links, and the most stable configuration was determined through testing.

Figure 4.2: Tank Tracks and Motors Individual Components and Fully Built.

Power Source

A 3-cell 18650 battery case was used, but the case does not connect the 3 cells in series. Wires were soldered to these connections so that there is only a positive and negative pin. Two sets of output wires were soldered to the case to be connected to the two buck converters. The ends of these wires were connected into the female of a molex connector (SP09). This is shown in Figure 4.3.

Figure 4.3: 3S 18650 Batteries in Case with Wiring

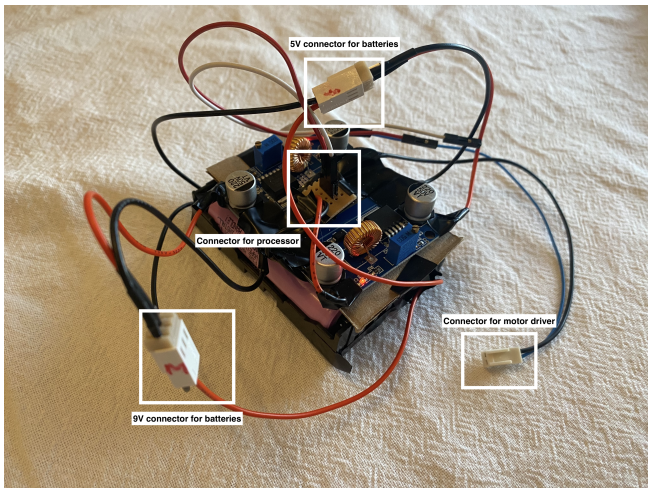

Figure 4.4: Buck Converters with Connectors

Buck Converters

Each buck converter was individually tested by applying a DC input and adjusting the onboard potentiometer to output 5V for the processor and 9V for the motor driver. The input voltage was varied to verify that the output remained stable under changing conditions. Wires were soldered to the input pins, and male Molex connectors were attached to allow the converters to be easily plugged in or disconnected from the power source (SP08).

For the 9V converter, the output wires were soldered to the board and the other end connected to female Molex connectors for connection to the motor driver. For the 5V converter, output wires were soldered to the board and were soldered to a veroboard, which was fitted with two female socket pins. This setup allowed jumper wires from the ESP32-CAM to be securely connected to the regulated 5V supply (SP09).

Motor Driver

The motor driver was tested with a 9V input and varying 2.8V PWM signals with varying duty cycles to confirm correct operation. Output voltage were measured and applied to the motor to verify current drawn under motor load. All connections were soldered based on Table 4.8 and the motor driver with the connections is shown in Figure 4.5 (SP09).

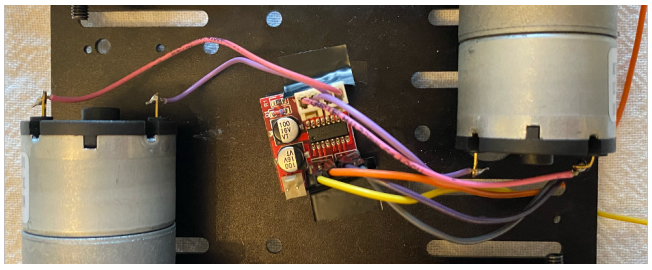

Figure 4.5: Motor Driver with Connections

Scooper Motor Connections

The two servo motors each have a ground, 5V, and signal wire connected via attached female jumpers. Because the ESP32-CAM does not support both servos directly, a connection hub was built using a veroboard with 2 male 3-pin headers and 4 female sockets (SP09). This shared the power and

Table 4.8: Motor Driver Pin Connections

Motor Driver Pin	Connection to	Type of Connector
Input positive	Voltage regulator output	Molex male connectors on the motor driver to female Molex connectors attached to the output of the 9V buck regulator's wires.
Input negative	Voltage regulator ground	
INT 1	ESP32-CAM GPIO 12	Female socket headers were used for male to female jumper headers to connect to the processor's female pins.
INT 2	ESP32-CAM GPIO 13	
INT 3	ESP32-CAM GPIO 14	
INT 4	ESP32-CAM GPIO 15	
Motor A positive	Right motor positive	Male Molex connectors were used. Wires were soldered to the motor pins with female Molex connectors on the end for this to be connected.
Motor A negative	Right motor negative	
Motor B positive	Left motor positive	
Motor B negative	Left motor negative	

ground while keeping independent signal lines. Figure 4.6 shows this connection board. It shows three connections points, although only two are used as early design were considering using 3 scooper motors.

Figure 4.6: Scooper Motor Connections

4.4.2 Failure Management

The system was designed for modularity and ease of maintenance, with all components connected using detachable connectors to allow quick disassembly and replacement if needed. Electrical insulation tape was applied to exposed connections to prevent short circuits and improve safety. Components were sourced locally within South Africa to ensure replacements are affordable, easily available, and reduce potential downtime.

4.5 Testing and Results

The complete compiled subsystem is shown in Figure 4.7.

Table 4.10 shows the acceptance tests for this subsystem and Table 4.9 shows the results of the testing.

The system successfully passed 10 out of the 11 defined Acceptance Test Procedures (ATPs), indicating strong overall performance and reliability. The only unmet requirement was ATP03, which evaluated

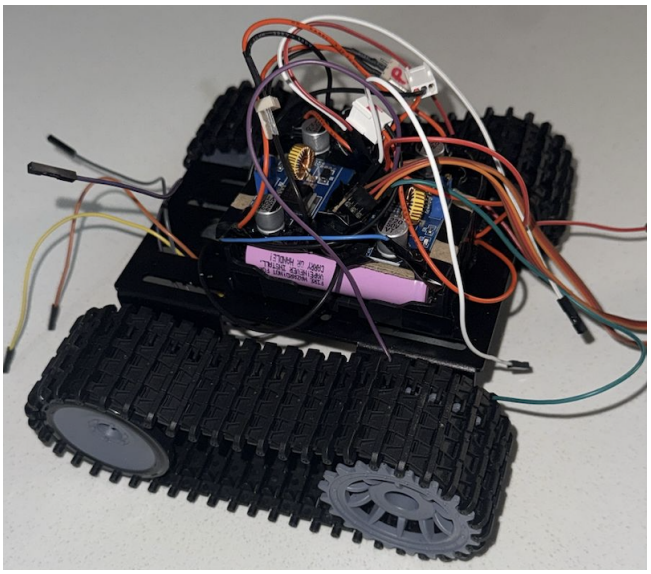

Figure 4.7: Electrical and Locomotion Subsystem

Table 4.9: ATP Summary Results

ATP ID	Result	Pass/Fail
ATP01	Motor was able to lift 0.5kg	Pass
ATP02	System was able to handle 5kg with no deformation	Pass
ATP03	Robot was able to operate up a 5 degree incline and over a 1cm obstacle.	Fail
ATP04	Motor responded to PWM in less than half a second.	Pass
ATP05	The ouput of the regualtors was 5V and 9V	Pass
ATP06	Power system operated reliably under full load.	Pass
ATP07	System operates at a maximum continuous current of 400mA and battery capacity is 3700mAh. Operates for more than 1 hour.	Pass
ATP08	Manual disconnection cuts power to the system.	Pass
ATP09	All connectors remain intact and secure	Pass
ATP10	Motor mounts remain firmly mounted after stress.	Pass
ATP11	Covered 2 meters in 10 seconds giving it a speed of 0.2m/s	Pass

the robot's ability to traverse a 15° incline and overcome a 2cm obstacle. This limitation likely stems from inadequate traction from the tank tracks or insufficient torque from the motors. Tank tracks were chosen for their superior stability and traction when using two motors; however, limited availability in South Africa restricted access to higher-performance options. In addition, the material constraints of the available 3D printer prevented the fabrication of improved custom tracks. With access to a more advanced 3D printer, more effective tracks could potentially be produced within the existing budget. Furthermore, the motors currently operate at 70% speed to maintain consistent movement. Future improvements could include dynamic speed control, allowing the system to increase power when needed to overcome more demanding terrain, which could enable the robot to meet ATP03.

4.6 Conclusion and Recommendations

The electrical and locomotion subsystem successfully integrates key components—motors, tank tracks, power source, motor driver, and regulators—into a robust platform that meets the majority of design and functional requirements. Ten out of eleven acceptance tests were passed, confirming the system's

Table 4.10: Acceptance Test Procedures with Pass/Fail Criteria

ATP ID	**Test Description**	**Pass/Fail Criteria**
ATP01	Attach a string with a radius of 6.5cm to the motors with a 0.5kg weight at the end. Apply 9V to the motors with this attached.	Motor are able to lift the load, therefore, torque $\geq 0.3Nm$. ($\tau = r \cdot m \cdot g$)
ATP02	Place a 3 kg load on the system when stationary and observe wheel/track integrity.	No visible deformation or mechanical failure. Structure supports load without collapsing.
ATP03	Operate robot up a 15° incline and over 2 cm obstacle. Observe traction and movement.	Robot ascends ramp and crosses obstacle without manual aid. No slipping or tipping.
ATP04	Send PWM command to control the motors. Measure the time taken for the motor to respond to the signal by video recording the signal and the motion of the motors in the same frame.	Motor begins motion within 1 second of PWM signal.
ATP05	Power the processor and motors using the power source (with voltage regulators). Measure the voltage at the input to the processor and motors using a voltmeter.	Processor receives 5V and motors receive 9V.
ATP06	Power the processor and motors using the power source. Keep the system under full load for at least 5 minutes and monitor the system.	The power source operates reliably with no significant overheating or damage.
ATP07	Power the system using the DC power supply. Operate the system to measure the maximum continuous current drawn from the power source.	Based on the capacity of the power source, and current drawn it is able to operate the system continuously for $\geq$ 1 hour without needing recharge.
ATP08	Power the system using a DC power source and use manual disconnection to cut power during operation. Confirm all subsystems shut off by ensuring that current drawn is $\leq$ 1mA.	Entire system powers down instantly when wires disconnected and voltage measures zero.
ATP09	Observe connectors during system vibration moving on an uneven surface and movement test. Inspect for loosening or disconnection.	No connectors come loose or disconnect. All connections remain intact and secure.
ATP10	Visually and physically inspect motor mounts. Apply vibration by moving system over an uneven surface. Check for looseness.	Motors remain firmly mounted after stress. No bolts/nuts/screws loosen.
ATP11	Drive system on a flat surface applying the maximum duty cycle of the PWM signal sent to the motors (70%). Measure the time it takes to travel 2 meters to calculate its speed.	Locomotion system reaches or exceeds 0.3 m/s.

reliability, adequate power delivery, and secure integration. The only limitation identified was the vehicle's inability to navigate a 15° incline and a 2cm obstacle, attributed to restricted traction and torque. To improve this, it is recommended that future iterations explore enhanced track designs using advanced 3D printing materials and incorporate dynamic motor control to provide adaptive torque during demanding conditions. These adjustments would improve terrain performance while maintaining the system's affordability and modularity.

Chapter 5

Control Subsystem

5.1 Introduction

The control subsystem of the guano scooping robot functions as the central control unit, coordinating both the robot's spatial motion and scooping operations while facilitating a real time video feedback stream. The subsystem enables remote control of the robot via a web-based graphical user interface (GUI) and provides control signals to the motors to facilitate their movement using a processor. These capabilities collectively allow a user to handle the system remotely by navigating the robot and collecting the required guano samples.

5.2 Requirements

The subsystem was designed with direct reference to the broader system's user requirements (URs), which lead to the specific functional requirements (FRs) in Table 5.1 and specification-level requirements (SPs) in Table 5.2. These requirements shaped all design decisions and testing procedures for the control subsystem.

Table 5.1: Functional Requirements

UR ID	**FR ID**	**Functional Requirement**
UR03	FR01	Remote operation of the robot's motion using a stable access network
UR05	FR02	Provide a live camera stream to aid navigation control
UR03	FR03	Enable directional movement control remotely
UR04	FR04	Enable remote actuation of the scooping mechanism
UR07	FR05	Provide a user-friendly GUI accessible by non-technical users to operate the robot
UR09	FR06	Ensure safe behaviour on connection loss or system fault

Table 5.2: Specifications Linked to Functional and User Requirements

Spec ID	**Specification**	**Linked FR(s)**	**ATP ID**

SP01	Processor can support connection over Wi-Fi or Bluetooth.	FR01	ATP01
SP02	Processor can interface with a compatible camera module.	FR02	ATP02
SP04	Provide control signals to the 4 input pins on the TC1508A H-bridge motor driver.	FR03	ATP04
SP05	Provide PWM signals to the servo motors FS90 to operate the arms at specific angles for scooping samples.	FR04	ATP05
SP06	The firmware must support programming interfaces for navigation and scooper control.	FR03, FR04, FR05	ATP06
SP08	Integrate a live camera stream with at least 480p resolution at 15 fps.	FR02	ATP07
SP09	The GUI must allow for directional control, stop, and sample collection through user inputs.	FR03, FR04, FR05	ATP08
SP10	The controller must handle safe reinitialization on start-up or network failure.	FR06	ATP09

5.3 Design Choices

5.3.1 Processor

The processor is the core of the control subsystem, acting as the command-and-control unit for both robot motion, sample collection and interfacing with the camera over a wireless network. The choice of the processor is critical as it impacts the robot's responsiveness, power consumption, GPIO availability and as a result the robot's overall functional capabilities. Table 5.3 shows the three most suitable processors for this subsystem.

Table 5.3: Comparison of Microcontroller Boards with Camera Support

Aspect	**ESP32-CAM**	**Raspberry Pi Pico W with Separate Camera**	**ESP32-S3-CAM**
Description	ESP32-S chip, OV2640 camera, Wi-Fi, Bluetooth, microSD card slot	RP2040 chip, 2.4 GHz Wi-Fi. Separate camera module required	ESP32-S3 chip, camera, Wi-Fi, Bluetooth 5.0 (BLE)
Cost	R160 – R200	Pico W: R150–R200 + cost of separate camera	R200 – R250
Processing Power	32-bit Dual-core 240MHz with onboard 520kB SRAM and external 2MB PSRAM	Dual-core 133MHz with 264kB SRAM and 2MB QSPI Flash	32-bit Dual-core 240MHz with 512kB SRAM, 384kB ROM, 8MB PSRAM, 16MB SPI Flash

Usable GPIO Pins	6 GPIO pins	26 GPIO pins	21–26 GPIO pins blank
Camera Interface	Integrated OV2640	Requires separate compatible camera module	Integrated (OV2640 or OV5640)
Wireless Connectivity	Wi-Fi (802.11 b/g/n), Bluetooth 4.2	Wi-Fi (802.11 b/g/n), Bluetooth 5.2	Wi-Fi (802.11 b/g/n), Bluetooth 5.0 BLE
Programming	Arduino IDE (requires USB-to-serial adapter)	Micro USB	Varies (some models have USB-C)
Size and Weight	27 × 40.5 mm, 20g	21 × 51 mm + separate camera, 4g	13 × 50.1 mm, 11g
Power Consumption	180mA to 310mA with flash	50mA to 150mA peak	90mA to 340mA
Input Voltage	3.3V to 5V DC	1.8V to 5.5V DC	3.3V to 5V DC

The ESP32-CAM's specifications, as detailed in the component comparison table, make it a suitable choice for this application. Its integrated Wi-Fi and camera reduce complexity and cost (SP01, SP02), while its processing power is sufficient for the required tasks (SP06). While it has a limited number of GPIO pins, it is sufficient for the basic motor control requirements of this project (SP03, SP04) as it has six usable GPIO pins available. The cost-effectiveness of the ESP32-CAM is also a significant advantage, ensuring the design adheres to budgetary constraints. Alternatives like the ESP32-S3-CAM and Raspberry Pi Pico W were considered, but the ESP32-CAM was chosen due to its cost-effectiveness and the integrated camera, which aligns with the project's constraints.Other processors, like the broader Raspberry Pi family, offer more power but at a higher cost and with unnecessary features for this project.

5.3.2 Navigation control

The motor control signal is designed to drive two DC motors using the TC1508A dual H-bridge motor driver, as required for enabling directional movement control remotely (FR03). Control signals are generated from the four GPIO pins on the ESP32-CAM: GPIO12 and 13 for the left motor and GPIO14 and 15 for the right motor as can be seen in Figure **??**. These pins are selected as they are safe to use for signal generation and do not connect to any other on-board processor modules, satisfying the requirement to provide control signals to the TC1508A motor driver (SP04).

For the signal type, both simple HIGH/LOW logic and PWM-based control were considered. While digital logic offers simplicity, it causes abrupt motion transitions and lacks fine control. PWM, in contrast, enables smoother motion through duty cycle modulation. The PWM-based design is chosen as it allows the signal to gradually increase the duty cycle of the motors from zero to maximum, preventing current surges and improving mechanical stability. The duty cycle is increased from zero to approximately 70% to accommodate for the uneven terrain in areas like Betty's Bay, therefore providing smoother and more stable motion. This implementation aligns with the requirement to support firmware interfaces for navigation control (SP06).

The navigational motion supports linear movement forwards (F) and backwards (B), including turning left (L) and right (R) capabilities. Table 5.4 describes the turning strategies considered for this design.

Table 5.4: Comparison of Robot Turning Control Options

Option	Description	Pros	Cons
Option 1	Robot turns with a single 90-degree motion and resumes forward movement.	- Intuitive directional control	- Requires precise timing and state to tracking to align angles
Option 2	Diagonal turning functionality (e.g. F-L, F-R, B-L, B-R).	- More motion states allow easier directional control, especially during backward motion	- Less control over turning angles unless implemented with hardware feedback - Cluttered GUI with too many options if using buttons
Option 3	Continuous rotation for L, R command until an interrupt is received.	- Precise control over turning angles allowing smoother arcs	- Must manually stop robot or it keeps spinning

Option 3 was chosen for its flexibility and ability to support real-time navigation by manually aligning the scooper with a target sample. This allows more accessibility to samples despite requiring precise user input to stop the motors from turning continuously. To maintain safety the stop functionality is implemented as an immediate stop, setting all outputs to LOW to immediately halt the motion on command if required.

5.3.3 Scooping motion control

The robot's scooping functionality to collect the penguin guano samples requires smooth and synchronous operation of the two servomotors to prevent the displacement of collected samples and ensure consistent operation over repeated cycles (FR04, SP05). The ESP32-CAM microcontroller interfaces with two servo motors via GPIO2 and GPIO 4, with their signals mirrored to each other as the servos are connected on the opposite sides of the robot.

To enable smooth, non-disruptive motion the angles of the servos needs to be gradually changed at steadily implemented time steps, providing gradual PWM transitions to signal the servos (SP06). The servo on GPIO 2 is written to angle θ, while the servo on GPIO 4 is written to θ, achieving symmetrical motion without requiring explicit feedback.

The collection movement begins with the servos rotating to lower the scooper arms to the ground with an angle of hein's section, followed by a short forward motion to ensure the sample has been scooped and then the arms return back to their initial position to not obstruct the camera and carry the sample safely (FR04). This logic mimics the motion of removing guano from a surface and accommodates for sample collection accuracy and reduced mechanical stress through simple motions.

GPIO2 is selected as it supports clean PWM output while GPIO4 was chosen as a design necessity to accommodate the two scooping arms. Due to the hardware-level binding of the on-board flash LED to GPIO 4 it could not be dimmed or set off while still providing stable scooping motion control. This trade-off is accepted due to limited available GPIO pins, and as the electrical subsystem can successfully handle current draw (SP05).

5.3.4 Programming Environment

The programming environment defines how the ESP32-CAM firmware is developed, compiled and deployed. The architecture must be lightweight, responsive and capable of supporting both low-level hardware control and high-level interface logic (SP06, FR05).

Table 5.5: Comparison of ESP32 Development Platforms

Category	**Arduino IDE (Selected)**	**PlatformIO (VS Code)**	**ESP-IDF (Espressif SDK)**
Ease of Use	Very beginner-friendly; minimal setup; fast testing	Moderate — requires extension setup, config files	Advanced — steep learning curve with CMake, partitioning, and config menus
Library Support	Strong support for ESP32-CAM (`esp_camera`, `WiFi`, `ESP32Servo`)	Similar library support; integrates with Arduino core	Full low-level control; requires direct driver management
Development Workflow	Single `.ino` sketch; no directory overhead	Structured project with `.cpp/.h` files; better modularity	Complex project with multiple CMake files; supports FreeRTOS
Debugging Tools	Basic serial monitor only	Integrated debugger (with compatible hardware); better code navigation	Full GDB support, tracing, task debugging
Build System	Simple click-to-compile	Task-based with auto environment management	Manual control via `idf.py` or CMake
Hardware Access Control	Abstracted through libraries (e.g., `analogWrite`, `servo.write`)	Same as Arduino core; supports hardware abstraction	Direct hardware register access
Languages Supported	C/C++, HTML, CSS, JS (served via Arduino IDE)	C/C++, HTML, JS (modularised in PlatformIO)	C/C++ only (frontend must be externally handled)
Deployment Speed	Fast flashing via FTDI/UART	Slightly slower due to task management overhead	Longer due to build complexity
Community Support	Large community, extensive tutorials for ESP32-CAM	Growing community; good PlatformIO/ESP32 docs	Mostly professional/industrial developers

For this project, the ARDUINO IDE was selected due to its simplicity, strong ESP community support and ease of integration with hardware level libraries such as for the GPIO pin controls, camera streaming and wireless network connectivity. While Platform IO and ESP-IDF provide a more structured and modular project setup, they introduce significant overhead which is unnecessary for the scope of this project. It enables the use of frontend web technologies (HTML, CSS, JS) embedded within the firmware. The Arduino IDE with its extensive library support fulfils all functional requirements of the control subsystem (FR01, FR02, FR03, FR04, FR05, FR06). Moreover, the platform's simple sketch format is efficient for rapid prototyping and easier debugging using the debugger which is extensively used in the code base. Moreover, with the limitation of development time, ARDUINO IDE has a low barrier to entry so it is easy for a beginner level embedded system programmer to understand.

Graphical User Interface(GUI) and visual feedback

User interface and visual feedback systems function as the central control interface to operate the robot remotely while maintaining spatial awareness through a live stream (FR02, FR05). Together they provide a responsive and low-complexity interaction model suitable for both field testing and conservation environments.

The GUI layout designs considered are described in Table 5.6. Add images in appendix

Design Option	Description	Pros	Cons
Option 1: Grid layout (Selected)	Four directional buttons (↑↓←→) arranged around a central stop button; "Collect Sample" button placed below	Intuitive spatial mapping Keyboard-friendly Easy to read	Takes more vertical space
Option 2: Vertical or Horizontal control simple control menu	Buttons placed in a single column or row	Compact and mobile-friendly	Less spatially intuitive
Option 3: Joystick-style interafce	Smooth control for experienced users	Difficult to operate on a non-touch screen	

Table 5.6: Comparison of GUI Design Options

The selected D-pad layout as seen in Figure was implemented using HTML/CSS and embedded directly into the ESP32 firmware. The GUI also includes a status box that confirms command responses, a WiFi status update and displays robot's state of motion. Keyboard support is implemented for key inputs such as arrow keys (for movement), spacebar (stop), and c (scooping) for easy control. The interface is highly reliable and simple with the style reflecting the context of the problems through the icons and the use of cool colours (FR05, SP09).

The live video streaming was implemented as a separate component window. Early designs which included the MJPEG streaming in the main GUI degraded the responsiveness of the interface due to

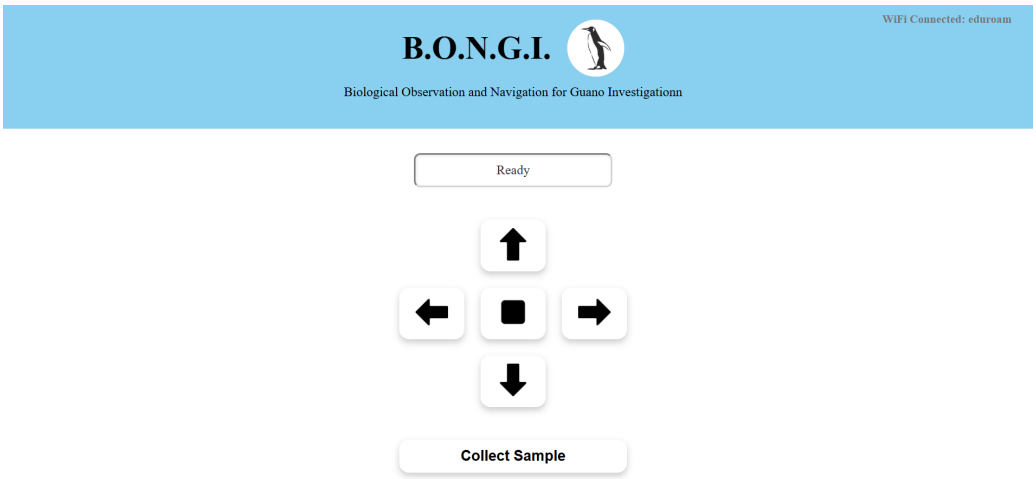

Figure 5.1: Graphical user interface alongside the camera stream

the nature of the ESP32's web server and the ESP's processing power. A similar result was obtained when implementing an asynchronous web server on the main control GUI. Hence, the selected approach was to use a standalone Python script that polls the image capture end point from the ESP server using JPEG frames which are combined as an MPJPEG stream using OpenCV. This script must however be manually run in a Python environment using a laptop or Field PC with preset libraries. While this affects the non-technical user access requirements, it is deemed as an acceptable design choice to maintain system responsiveness especially when handling high sensitivity operations like scooping control (FR02, FR05). The Python script is run with minimal complexity and launches the camera stream without affecting the ESP32's processing capabilities significantly. The script is also saved with a date attached to it for future access (SP08).

Communication Modes

The communication architecture uses Wi-Fi-based HTTP to transmit user commands and relay visual feedback from the ESP32-CAM. Once connected to a local or institutional network, the ESP32 hosts a synchronous web server on port 80 to serve the GUI, handle HTTP GET requests, and provide the endpoint for sending images at its end point (FR01, FR02, SP01).

Alternative modes were considered. Bluetooth offered offline pairing but lacked range, browser support, and streaming capability. Operating the ESP32 as a Wi-Fi access point was also explored but was limited by short range and loss of online GUI assets. Wi-Fi client mode was selected for its ease of set-up, multi-device access, browser compatibility, and sufficient responsiveness for GUI control and visual feedback (SP11).

5.4 Sub-Module Design

The controller subsystem consists of five primary software driven submodules: motor control, servo control, graphical user interface (GUI), camera streaming, and communication network. Each of these submodules interfaces directly with the ESP32-CAM, forming a cohesive firmware system that provides full remote operational control on th robot over WiFi. The interfacing diagram shown in Figure 5.2 provides an overview of the processor interfaces with the rest of the system.

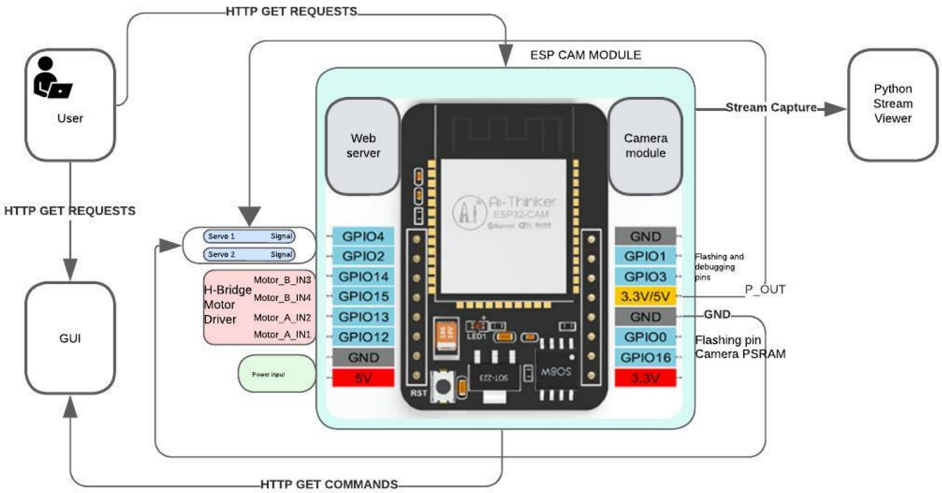

Figure 5.2: Interfacing diagram of the processor with robot's hardware and software components

5.4.1 Motor control

The motor control submodule drives two DC motors via a TC1508A H-bridge using GPIO 12–15 on the ESP32-CAM. Each motion command is mapped to a stateless HTTP GET endpoint, which triggers a rampMotors() and rampTurn() function to gradually increase PWM duty cycle for smooth acceleration. All motion functions are stateless, ensuring the most recent command takes effect. A stopMotors() function sets all outputs LOW to halt motion safely. Output signals were verified using an oscilloscope, with with ramping and direction changes tested via the GUI (after GUI based ATP blank passed).

5.4.2 Servo motor control

This submodule handles the generation of abstract low level PWM signals t control two synchronized FS90 servos which to actuate a scooping motion. The smoothMove fucntion gradually interpolates between angles at set delays to ensure gradual arm motion. The signal integrity of GPIO2 and GPIO4 is tested using an oscilloscope and system response logs.

5.4.3 GUI and camera streaming

The GUI is served from the ESP32-CAM using embedded HTML and JavaScript. Button clicks and keyboard inputs send HTTP GET requests for movement, stopping, and scooping. The /capture endpoint provides a single-frame JPEG stream, which is polled by an external Python script to display a live video feed. The GUI and camera stream were intentionally separated to maintain responsiveness. Both subsystems were verified through command response testing on the GUI serial monitor and verified with real-time operation.

5.4.4 Communication mode

The ESP32-CAM operates as a Wi-Fi client on a WPA2 Enterprise network, hosting a synchronous web server to serve the GUI, process HTTP GET commands, and provide the /capture endpoint. All communication is stateless, ensuring consistent behaviour even with rapid input or reconnects. This

setup enables reliable multi-device access and offloads streaming to an external client.

5.5 Testing and Results

The control subsystem was tested modularly using the Acceptance Test procedures (ATPs) detailed in Table 5.7. Motion and scooping signals were validated via GPIO output states and PWM signal behavior, while GUI functionality was tested through both mouse and keyboard inputs. Camera feedback was assessed using a custom Python script that polled the /capture endpoint at real-time intervals. Network connection stability, stateless command handling, and system recovery from reboot or disconnection were also verified.

Table 5.7: Control Subsystem Acceptance Test Plan

ATP ID	**Test Description**	**Test Method**	**Pass Criteria**
ATP01	Connect to a wireless network hotspot and check server load response	Power on ESP board, load the server IP	Page loads successfully and GUI is accessible in browser
ATP02	Test control signal output for motor control (directional)	Send direction commands from GUI and test output signal at GPIO pin 12,13 for motor A and 14,15 for motor B	Expected PWM signal output on each pin changes depending on direction command
ATP03	Observe PWM ramping behavior	Use oscilloscope on GPIO 12–15 during ramp and give direction commands	PWM ramps up smoothly to maximum duty cycle
ATP04	Test emergency stop function	Send stop command during motion	All motors stop with an immediate response
ATP05	Execute scooping motion	Send Collect Sample command, observe GPIO 2/4 PWM output	Servo arms sweep smoothly, then reset
ATP06	Servo initialization test	Power on board, observe servo output or position	Servos initialize to 90° (mirror)
ATP07	GUI button responsiveness	Click GUI buttons and observe serial monitor output	Each button gives expected function invoked
ATP08	GUI keyboard control test	Use arrow keys and C/space on GUI	Correct endpoints triggered
ATP09	Test camera stream	Run Python script when server active	Real-time camera stream displayed
ATP10	Test camera stream save	End running camera script	Check destination directory and verify stream captured
ATP11	MJPEG stream performance	Run Python script and check GUI responsiveness	∼15 FPS; no GUI lag or freeze

ATP12	Command stateless behavior	Change commands when operating	Only latest command active; no lock-up
ATP13	Reboot behavior check	Power cycle ESP32-CAM, reload GUI	System reconnects, servos reinitialize
ATP14	Remote-only operation check	Run system fully from GUI with no physical interaction	All features operable remotely
ATP15	Multi-function load test	Stream video + run motion + scoop commands simultaneously	No ESP crash or loss of responsiveness
ATP16	GPIO state on startup	Probe GPIO 12–15, 2, 4 on power-up before commands sent	No active motion signal before user input
ATP17	GUI command echo	Trigger commands and read GUI status box + Serial	Status feedback shown; logs confirm endpoint hit
ATP18	GUI reload test	Refresh browser or reset ESP during use	GUI reloads and remains operable
ATP19	Environmental compliance: low noise and no disruptive lighting	Run system in controlled setting; observe LED flash and motor/servo sound levels	System operates quietly and without visible light disruption
ATP20	Components within budget	System operates quietly and without visible light disruption	

All control subsystem tests listed in Table 5.7 were successfully completed. The ESP32-CAM processor responded correctly to all GUI commands, including motor control, servo sweeping, and remote operation. Directional movement commands triggered the correct GPIO outputs, and the PWM ramping behaved as expected with no stalling or overshooting ([ATP02], [ATP03]).The servo scooping sequence also worked reliably with no jitter or delay after tuning the delay step to 25 ms ([ATP05], [ATP06]). Camera streaming from the ESP32 to an external Python client was verified to operate at roughly 15 FPS, while GUI controls remained responsive throughout ([ATP09], [ATP11]). Stream capture also functioned correctly when manually stopped ([ATP10]).

The system passed all interface and usability tests. Emergency stop commands were processed immediately ([ATP04]), keyboard and button commands triggered the correct actions ([ATP07], [ATP08]), and the GUI echoed back command responses via the status display ([ATP17]). The GUI remained functional after browser refresh or ESP reset ([ATP18]), and full remote operation was confirmed ([ATP14]).Stability was verified under multi-function load, where streaming, motor control, and servo operation occurred concurrently without system crash ([ATP15]). GPIOs were also confirmed to remain inactive on power-up, preventing unwanted motion ([ATP16]).

ATP19 failed as was the onboard flashlight LED, which remained ON during the entire processes.

While it does not affect functionality, this may be distracting in high sensitivity environments like in this project.

5.6 Conclusion and Future recommendations

The control subsystem for the penguin guano collection robot met all key requirements, demonstrating reliable motor and servo control, GUI responsiveness, and external camera streaming. The ESP32-CAM, programmed via the Arduino IDE, successfully handled GPIO-based motion commands, while the web-based GUI allowed intuitive remote operation with both button and keyboard inputs. A hardware-related issue was observed: the onboard LED flashlight remained on during servo operation, due to pin overlap with the servo GPIO. Additionally, streaming was intentionally offloaded to an external Python client after tests showed that running both control and video on a single server led to UI freezing and lag. This design choice preserved system responsiveness and allowed smooth real-time streaming. Future work may include integrating asynchronous web server functionality for unified streaming and control, enhancing GUI feedback with more system acess security measures, and linking the external vision module to support semi-autonomous scooping or navigation suggestions based on object detection. Overall, the subsystem is robust, effective, and well-positioned for future expansion.

Chapter 6

Conclusions

The purpose of this project was to...

This report began with...

The literature review was followed in Chapter...

The bulk of the work for this project followed next, in Chapter...

In Chapter...

Finally, Chapter... attempted to...

In summary, the project achieved the goals that were set out, by designing and demonstrating...

Chapter 7

GA Requirements

Subsystem Title	[Insert Rachael's Subsystem Title]
Student Number	GSBRAC001
GA 3: Engineering Design	Section **Design Choices** and **Submodule Design**, pages XX–YY
GA 7: Sustainability and Impact of Engineering Activity	D-School sessions, Section **Design Refinements and Optimisations**, pages XX–YY
GA 8: Individual, Team and Multi-disciplinary Working	See Teams group for meeting minutes
GA 10: Engineering Professionalism	All submission activities met, including report, presentation, and meeting deadlines

Table 7.1: Graduate Attributes Mapping – Rachael Guise-Brown (GSBRAC001)

Subsystem Title	[Insert Kavya's Subsystem Title]
Student Number	KSHKAV001
GA 3: Engineering Design	Section **Design Choices** and **Submodule Design**, pages XX–YY
GA 7: Sustainability and Impact of Engineering Activity	D-School sessions, Section **Design Refinements and Optimisations**, pages XX–YY
GA 8: Individual, Team and Multi-disciplinary Working	See Teams group for meeting minutes
GA 10: Engineering Professionalism	All submission activities met, including report, presentation, and meeting deadlines

Table 7.2: Graduate Attributes Mapping – Kavya Kaushik (KSHKAV001)

Subsystem Title	Chassis and Scraper Subsystem
Student Number	CRSHEI004
GA 3: Engineering Design	Sections **Design Choices** (p. 23), **Submodule Design** (p. 27), and **CAD Modelling and Simulation** (p. 29)
GA 7: Sustainability and Impact of Engineering Activity	Sections **Design Refinements and Optimisations** (p. 34), **Material Choice** (PLA, reuse of ice cream tub), and **Colour Consideration** (black for environmental blending)
GA 8: Individual, Team and Multi-disciplinary Working	Contributions recorded in Teams group, individual subsystem authored and presented
GA 10: Engineering Professionalism	Final report authored and submitted on time, subsystem presented and documented according to guidelines

Table 7.3: Graduate Attributes Mapping – Heinrich Crous (CRSHEI004)

Bibliography

[1] F. Schmitz and P. Wagner, "Moult phenology and the influence of breeding activity in adult african penguins spheniscus demersus at allwetterzoo münster, germany," *Journal of Zoo and Aquarium Research*, vol. 12, no. 2, pp. 125–132, 2024.

[2] J. Cooper, "Moult of the black-footed penguin spheniscus demersus," *International Zoo Yearbook*, pp. 22–26, 1978.

[3] L. J. Waller, "The african penguin spheniscus demersus: Conservation and management issues," Ph.D. dissertation, University of Cape Town, South Africa, 2011.

[4] R. J. M. Crawford, M. Hemming, J. Kemper, N. T. W. Klages, R. M. Randall, L. G. Underhill, A. D. Venter, V. L. Ward, and A. C. Wolfaardt, "Molt of the african penguin, spheniscus demersus, in relation to its breeding season and food availability," *Acta Zoologica Sinica*, vol. 52, no. suppl., pp. 435–439, 2006.

[5] L. M. Mazzaro, J. Meegan, D. Sarran, T. A. Romano, V. Bonato, S. Deng, and J. L. Dunn, "Molt-associated changes in hematologic and plasma biochemical values and stress hormone levels in african penguins (spheniscus demersus)," *Journal of Avian Medicine and Surgery*, vol. 27, no. 4, pp. 285–293, 2013.

[6] C. J. A. Austin, "Etiological study of molt abnormalities in the african penguin, spheniscus demersus," Bachelor's thesis, Butler University, Indianapolis, IN, USA, 2016.

[7] J. Roberts, "African penguin (spheniscus demersus) distribution during the non-breeding season: preparation for, and recovery from, a moulting fast," Master's thesis, University of Cape Town, South Africa, 2016.

[8] C. Hugo, "Investigating factors that influence the breeding success of the endangered african penguin (spheniscus demersus) at a mainland and island colony in the western cape, south africa," Master's thesis, University of the Western Cape, Cape Town, South Africa, 2022.

[9] J. Kemper, L. G. Underhill, J.-P. Roux, P. A. Bartlett, Y. J. Chesselet, J. A. C. James, R. Jones, N.-N. Uhongora, and S. Wepener, "Breeding patterns and factors influencing breeding success of african penguins spheniscus demersus in namibia," in *Top Predators of the Benguela System*, G. B. Crawford, Ed. Cape Town: Avian Demography Unit, University of Cape Town, 2007, pp. 89–96.

[10] T. Lewis, "Knowledge and attitudes of south african stakeholders regarding conservation of the african penguin (spheniscus demersus)," Master's thesis, University of Pretoria, South Africa, 2023.

[11] M. V. Driscoll, A. D. Tuttle, and T. A. Romano, "Fecal glucocorticoid analysis as a health monitoring tool for endangered african penguins (spheniscus demersus)," *General and Comparative Endocrinology*, vol. 330, p. 114147, 2023.

[12] N. J. Parsons, T. A. Gous, A. M. Schaefer, and R. E. T. Vanstreels, "Health evaluation of african penguins (spheniscus demersus) in southern africa," *Onderstepoort Journal of Veterinary Research*, vol. 83, no. 1, p. a1147, 2016.

[13] N. J. Parsons, A. M. Schaefer, S. D. van der Spuy, and T. A. Gous, "Establishment of baseline haematology and biochemistry parameters in wild adult african penguins (spheniscus demersus)," *Journal of the South African Veterinary Association*, vol. 86, no. 1, pp. 1–8, 2015.

[14] D. S. Reynolds and T. H. Kunz, *Body Composition Analysis of Animals: A Handbook of Non-Destructive Methods*. Cambridge University Press, 2001.

[15] J. Sears, "Assessment of body condition in live birds; measurements of protein and fat reserves in the mute swan (cygnus olor)," *Journal of Zoology*, vol. 216, pp. 295–308, 1988.

[16] C. Korine, S. Daniel, I. G. van Tets, R. Yosef, and B. Pinshow, "Measuring fat mass in small birds by dual-energy x-ray absorptiometry," *Physiological and Biochemical Zoology*, vol. 77, no. 3, pp. 522–529, 2004.

[17] C. G. Guglielmo, L. P. McGuire, A. R. Gerson, and C. L. Seewagen, "Simple, rapid, and non-invasive measurement of fat, lean, and total water masses of live birds using quantitative magnetic resonance," *Journal of Ornithology*, vol. 152, no. Suppl 1, pp. S75–S85, 2011.

[18] J. Claffy, "Small bird perch scale," 2002, unpublished technical document.

[19] D. F. Larios, C. Rodríguez, J. Barbancho, M. Baena, M. Leal, J. Marín, C. León, and J. Bustamante, "An automatic weighting system for wild animals based on an artificial neural network: How to weigh wild animals without causing stress," *Sensors*, vol. 13, no. 3, pp. 2862–2883, 2013.

[20] K. Kerry, J. Clarke, and G. Else, "The use of an automated weighing and recording system for the study of the biology of adélie penguins (pygoscelis adeliae)," *Proc. NIPR Symp. Polar Biol.*, vol. 6, pp. 62–75, 1993.

[21] A. Lescroël, A. Schmidt, M. Elrod, D. G. Ainley, and G. Ballard, "Foraging dive frequency predicts body mass gain in the adélie penguin," *Scientific Reports*, vol. 11, no. 22883, 2021.

[22] J. P. Hayes and J. S. Shonkwiler, "Morphometric indicators of body condition: Worthwhile or wishful thinking?" in *Body Composition Analysis of Animals: A Handbook of Non-Destructive Methods*. Cambridge University Press, 2010, pp. 1–23.

[23] R. B. Sherley, T. Burghardt, P. J. Barham, N. Campbell, and I. C. Cuthill, "Spotting the difference: towards fully-automated population monitoring of african penguins spheniscus demersus," *Endangered Species Research*, vol. 11, pp. 101–111, 2010.

[24] C. Southwell and L. Emmerson, "Remotely-operating camera network expands antarctic seabird observations of key breeding parameters for ecosystem monitoring and management," *Journal for Nature Conservation*, vol. 23, pp. 1–8, 2015.

[25] J. Zhang, X. Luo, C. Chen, Z. Liu, and S. Cao, "A wildlife monitoring system based on wireless image sensor networks," *Sensors & Transducers*, vol. 180, no. 10, pp. 104–109, 2014. [Online]. Available: http://www.sensorsportal.com/HTML/DIGEST/P_2446.htm

[26] S. Szabó and M. Alexy, "Practical aspects of weight measurement using image processing methods in waterfowl production," *Agriculture*, vol. 12, no. 11, p. 1869, 2022.

[27] F. Sardà-Palomera, G. Bota, C. Viñolo, O. Pallarés, V. Sazatornil, L. Brotons, S. Gomáriz, and F. Sardà, "Fine-scale bird monitoring from light unmanned aircraft systems," *Ibis*, vol. 154, no. 1, pp. 177–183, 2012.

[28] F. Geldenhuys, "Using species distribution models for spatial conservation planning of african penguins," Master's thesis, Stellenbosch University, Stellenbosch, South Africa, 2018, [Online]. Available: https://scholar.sun.ac.za.

[29] J. Zupan, "Introduction to artificial neural network (ann) methods: What they are and how to use them," *Acta Chimica Slovenica*, vol. 41, no. 3, pp. 327–352, 1994.